

# Switching Transferable Gradient Directions for Query-Efficient Black-Box Adversarial Attacks

Chen Ma  
mac16@mails.tsinghua.edu.cn  
School of Software, BNRist, Tsinghua  
University  
Beijing, China

Shuyu Cheng  
chengsy18@mails.tsinghua.edu.cn  
Dept. of Comp. Sci. and Tech., BNRist  
Center, Institute for AI, THBI Lab,  
Tsinghua University  
Beijing, China

Li Chen\*  
chenlee@tsinghua.edu.cn  
School of Software, BNRist, Tsinghua  
University  
Beijing, China

Jun Zhu  
dcszj@mail.tsinghua.edu.cn  
Dept. of Comp. Sci. and Tech., BNRist  
Center, Institute for AI, THBI Lab,  
Tsinghua University  
Beijing, China

Junhai Yong  
yongjh@tsinghua.edu.cn  
School of Software, BNRist, Tsinghua  
University  
Beijing, China

## ABSTRACT

We propose a simple and highly query-efficient black-box adversarial attack named SWITCH, which has a state-of-the-art performance in the score-based setting. SWITCH features a highly efficient and effective utilization of the gradient of a surrogate model  $\hat{g}$  w.r.t. the input image, *i.e.*, the transferable gradient. In each iteration, SWITCH first tries to update the current sample along the direction of  $\hat{g}$ , but considers switching to its opposite direction  $-\hat{g}$  if our algorithm detects that it does not increase the value of the attack objective function. We justify the choice of switching to the opposite direction by a local approximate linearity assumption. In SWITCH, only one or two queries are needed per iteration, but it is still effective due to the rich information provided by the transferable gradient, thereby resulting in unprecedented query efficiency. To improve the robustness of SWITCH, we further propose SWITCH<sub>RGF</sub> in which the update follows the direction of a random gradient-free (RGF) estimate when neither  $\hat{g}$  nor its opposite direction can increase the objective, while maintaining the advantage of SWITCH in terms of query efficiency. Experimental results conducted on CIFAR-10, CIFAR-100 and TinyImageNet show that compared with other methods, SWITCH achieves a satisfactory attack success rate using much fewer queries, and SWITCH<sub>RGF</sub> achieves the state-of-the-art attack success rate with fewer queries overall. Our approach can serve as a strong baseline for future black-box attacks because of its simplicity. The PyTorch source code is released on <https://github.com/machanic/SWITCH>.

## CCS CONCEPTS

• **Theory of computation** → **Adversarial learning**

## KEYWORDS

black-box adversarial attack; adversarial attack; query-based attack

## 1 INTRODUCTION

Adversarial attacks present a major security threat to deep neural networks (DNNs) by adding human-imperceptible perturbations

to benign images for the misclassification of DNNs. Adversarial attacks can be divided into two main categories based on whether the internal information of the target model is exposed to the adversary, *i.e.*, white-box and black-box attacks. Compared to white-box, black-box attacks are more useful because they do not require the parameters or gradients of the target model. The black-box attacks can be divided into transfer- and query-based attacks.

Transfer-based attacks generate adversarial examples by attacking a pre-trained surrogate model to fool the target model [11, 19, 25]. Such attacks have practical value because they do not require querying the target model. However, the attack success rate is typically low in the following situations: (1) targeted attack, and (2) the network structures of the surrogate model and target model have a large difference. The low success rate is mainly because the surrogate model’s gradient deviates too much from the true gradient. The former could frequently point to a non-adversarial region of target model, so following this direction consecutively leads to a failed attack. Hence, how to switch the gradient when it deviates from the correct direction is worthy of further exploration.

Query-based attacks require an oracle access to the target model, and we focus on the score-based attack setting which requires accessing to the loss function value. Some score-based attacks [7, 20, 21, 36] estimate an approximate gradient by querying the target model at multiple points. However, the high query complexity is inevitable in estimating the approximate gradient with high precision. To reduce the query complexity, another type of query-based attacks, *i.e.*, random-search-based attacks [3, 15], eliminates the gradient estimation and turns to sampling a random perturbation at each iteration, which is either added to or subtracted from the target image. Then, the perturbed image is fed to the target model to compute a loss value. If the loss value peaks a historical high, the adversary accepts the perturbation; otherwise, it is rejected. The main issue of this strategy is that the sampled perturbation does not incorporate the gradient information, thereby leading to a high rejection rate and inefficient optimization. In addition, nothing is done if the perturbation is rejected, resulting in many wasted queries. Thus, how to incorporate the gradient information to enhance the optimization’s efficiency should be investigated.

\*Corresponding author.

In this study, we propose a novel black-box adversarial attack named SWITCH that exploits and revises the surrogate model’s gradient (called surrogate gradient) to improve the query efficiency. The surrogate gradient is a promising exploration direction for *maximizing* the objective loss function<sup>1</sup>, but it does not always point the target model’s adversarial region. To detect such situation and reduce incorrect updates, SWITCH proposes to query a loss value  $\mathcal{L}(\mathbf{x}_{\text{adv}} + \eta \cdot \hat{\mathbf{g}})$  based on a temporarily generated image  $\mathbf{x}_{\text{adv}} + \eta \cdot \hat{\mathbf{g}}$  updated along the  $\ell_p$  normalized surrogate gradient  $\hat{\mathbf{g}}$ , where  $\eta$  is the step size. If this loss is not increased from the last iteration ( $\mathcal{L}(\mathbf{x}_{\text{adv}} + \eta \cdot \hat{\mathbf{g}}) < \mathcal{L}(\mathbf{x}_{\text{adv}})$ ), SWITCH considers switching to a new direction that is obtained by taking a negative sign for the surrogate gradient (namely  $-\hat{\mathbf{g}}$ ). The effectiveness of this opposite direction is based on the (local) approximate linearity assumption of DNNs [14]. However, the approximate linearity assumption may not always hold and then the  $-\hat{\mathbf{g}}$  may point to a worse direction. To prevent such situation, our algorithm queries the loss  $\mathcal{L}(\mathbf{x}_{\text{adv}} - \eta \cdot \hat{\mathbf{g}})$  and then selects a relatively better direction from  $\{-\hat{\mathbf{g}}, \hat{\mathbf{g}}\}$ . Specifically, we compare  $\mathcal{L}(\mathbf{x}_{\text{adv}} - \eta \cdot \hat{\mathbf{g}})$  with  $\mathcal{L}(\mathbf{x}_{\text{adv}} + \eta \cdot \hat{\mathbf{g}})$ , and the gradient direction ( $-\hat{\mathbf{g}}$  or  $\hat{\mathbf{g}}$ ) that corresponds the larger loss value will be taken as the final direction for the update. Note that this comparison cannot exclude the situation in which both  $\mathcal{L}(\mathbf{x}_{\text{adv}} + \eta \cdot \hat{\mathbf{g}}) < \mathcal{L}(\mathbf{x}_{\text{adv}})$  and  $\mathcal{L}(\mathbf{x}_{\text{adv}} - \eta \cdot \hat{\mathbf{g}}) < \mathcal{L}(\mathbf{x}_{\text{adv}})$  happen, and thus SWITCH cannot always increase the loss during the attack. To deal with this problem, we further propose an extended version of SWITCH, *i.e.*, SWITCH<sub>RGF</sub>.

SWITCH<sub>RGF</sub> makes up for the shortcoming of SWITCH. It adopts a more effective direction ( $\hat{\mathbf{g}}_{\text{RGF}}$ ) by using random gradient-free (RGF).  $\hat{\mathbf{g}}_{\text{RGF}}$  is an approximate gradient direction that is obtained by using a number of queries, but it can increase the loss value with a great probability if both  $\hat{\mathbf{g}}$  and  $-\hat{\mathbf{g}}$  fail. Therefore, SWITCH<sub>RGF</sub> improves the success rate over SWITCH.

Finally, the adversarial image is updated by using the selected direction. Thus, in each iteration, the algorithm aims to keep the loss function increasing by switching the gradient. Both the attack success rate and query efficiency are improved because the switched direction could avoid following the wrong direction and consequently bypass the potential obstacle in optimization.

We evaluate the proposed method on the CIFAR-10 [23], CIFAR-100 [23] and TinyImageNet [34] datasets and compare it with 7 state-of-the-art query-based black-box attacks. The results show that the proposed approach requires the fewest queries to achieve a high attack success rate, which significantly outperforms other methods. Therefore, SWITCH achieves new state-of-the-art performance.

The main contributions of this study are as follows.

(1) We propose a simple and highly query-efficient black-box attack named SWITCH that exploits and revises the surrogate gradient  $\hat{\mathbf{g}}$  during optimization. SWITCH tries to select a better direction in each iteration to avoid following the wrong direction, which keeps the objective loss function rising as much as possible.

(2) We also propose an extended version of our algorithm *i.e.*, SWITCH<sub>RGF</sub>, which further improves the success rate over SWITCH.

(3) Despite its simplicity, SWITCH and SWITCH<sub>RGF</sub> spend fewer queries than 7 state-of-the-art methods and significantly improves the attack success rate over the baseline on the CIFAR-10, CIFAR-100 and TinyImageNet datasets. We consider the proposed method to be a strong baseline for future attacks.

## 2 BACKGROUND

**Black-box attacks.** It is unrealistic to obtain internal information of target models in many real-world systems, thus many studies focus on performing attacks in the black-box setting. Black-box attacks can be divided into transfer- and query-based attacks. In transfer-based attacks [11, 19, 25, 32], adversarial examples generated by attacking a surrogate model might remain adversarial for the target model. Given that targeted attack is difficult for transfer-based attacks, certain methods use the ensemble of surrogate models [25] to improve the success rate. However, the attack success rate remains unsatisfactory and new types of attacks can be detected easily by using a meta-learning-based detector [28].

Query-based attacks can be further divided into decision- and score-based attacks based on the type of information returned from the target model to the adversary. In decision-based attacks [8, 13], the adversary only knows the output label of the target model. In this study, we focus on the score-based attack, in which the adversary can obtain the output scores of the target model. Although the true gradient cannot be directly obtained in black-box attacks, we can still optimize the adversarial examples by using the approximate gradients. Early studies [5, 7] estimate the approximate gradient by sampling from a noise distribution around the pixels, which is expensive because each pixel needs two queries. To reduce the query complexity, methods are improved by incorporating data and time prior information [21], using meta-learning to learn a simulator [27], searching the solution among the vertices of the  $\ell_\infty$  ball [30], and searching the adversarial perturbation on a low-dimensional embedding space [36]. Different from the methods that estimate gradients, random-search-based attacks [3, 15] sample a random perturbation with the values filled with the maximum allowed perturbation  $\epsilon$  or  $-\epsilon$ , which is either added to or subtracted from the target image. Then, the modified image is fed to the target model to determine whether to accept the perturbation. This type of methods significantly reduces the query complexity because they directly find the solution among the extreme points in  $\ell_p$  ball and do not require the high-cost gradient estimation. However, the sampled perturbation does not encode the gradient information, resulting in inefficient optimization. In contrast, the proposed method exploits the gradient of the surrogate model and then switches the direction when necessary to keep the loss increasing as much as possible, thereby achieving high success rate and query efficiency.

**Adversary Setup.** Given the target model  $f$  and input-label pair  $(\mathbf{x}, y)$ , which is correctly classified by  $f$ . The adversarial example  $\mathbf{x}_{\text{adv}}$  is produced by  $\mathbf{x}_{\text{adv}} = \mathbf{x} + \delta$  that satisfies  $\|\mathbf{x}_{\text{adv}} - \mathbf{x}\|_p \leq \epsilon$ , where  $\epsilon$  is a predefined maximum allowed distance, and  $\delta$  is a small perturbation. The goal is to find  $\mathbf{x}_{\text{adv}}$  that maximizes the attack objective loss function  $\mathcal{L}(\cdot, \cdot)$ , which can be the cross-entropy loss or the max-margin logit loss. The projected gradient descent (PGD) attack [29] iteratively updates adversarial examples as  $\mathbf{x}_{\text{adv}} \leftarrow \text{Clip}_\epsilon(\mathbf{x}_{\text{adv}} + \eta \cdot \hat{\mathbf{g}})$ , where  $\text{Clip}_\epsilon$  denotes the clipping operation to

<sup>1</sup>In this study, we maximize the attack objective loss function to update the adversarial example.

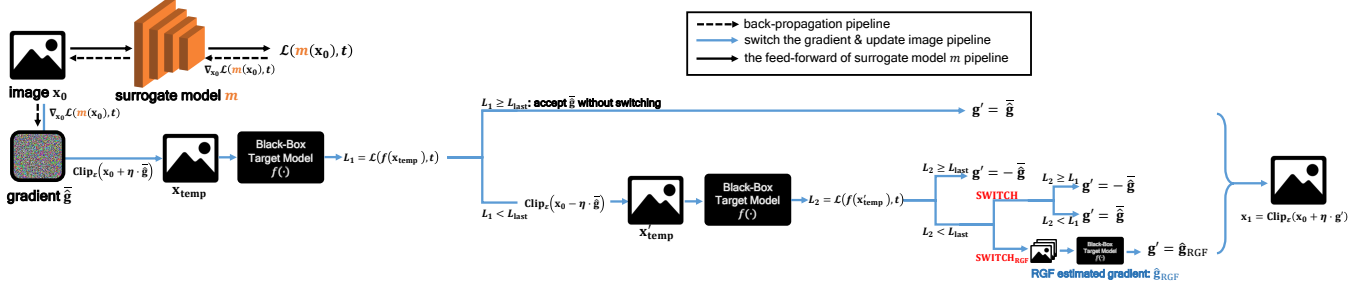


Figure 1: Illustration of an attack iteration (detailed in Algorithm 1), where  $L_{1\text{last}}$  indicates the loss value of the last iteration, and  $t$  indicates the target class in targeted attack and true class in untargeted attack. In each iteration, the algorithm makes a temporary image  $x_{\text{temp}}$  with the normalized surrogate gradient  $\bar{g}$ , namely  $x_{\text{temp}} = \text{Clip}_\epsilon(x_{\text{adv}} + \eta \cdot \bar{g})$ . Then, the loss  $L_1$  is computed by feeding  $x_{\text{temp}}$  to the target model. If  $L_1 \geq L_{1\text{last}}$ , the algorithm accepts  $\bar{g}$ . Otherwise, the gradient  $\bar{g}$  deviates too much from the true gradient such that  $L_1 < L_{1\text{last}}$ . Then we switch to the direction of  $-\bar{g}$  and query a loss value  $L_2$  based on another temporary image  $\text{Clip}_\epsilon(x_{\text{adv}} - \eta \cdot \bar{g})$ . After the feedback is obtained, we consider two options, namely, SWITCH and its extended version SWITCH<sub>RGF</sub>. SWITCH selects a direction from  $\bar{g}$  and  $-\bar{g}$  that corresponds to the larger loss value between  $L_1$  and  $L_2$  as the final direction  $g'$ . SWITCH<sub>RGF</sub> turns to using RGF to estimate an approximate gradient as  $g' = \hat{g}_{\text{RGF}}$  if both  $L_1$  and  $L_2$  are less than  $L_{1\text{last}}$ . Finally, the sample  $x_1$  is generated by using  $g'$ .

restrict images within a  $\ell_p$  ball centered at  $x$  with the radius of  $\epsilon$ ;  $\eta$  is the learning rate;  $g = \nabla_{x_{\text{adv}}} \mathcal{L}(f(x_{\text{adv}}), y)$  is the gradient of the objective loss function at  $x_{\text{adv}}$ ; and  $\bar{g}$  denotes a normalized version of  $g$  under  $\ell_p$  norm, i.e.,  $\bar{g} = \frac{g}{\|g\|_2}$  under  $\ell_2$  norm and  $\bar{g} = \text{sign}(g)$  under  $\ell_\infty$  norm. In this study, we also follow above steps to update the adversarial image, except that we do not have access to the true gradient  $g$  in the black-box setting and replace it with a suitable direction  $\hat{g}$ .

### 3 METHOD

The proposed algorithm is illustrated in Fig. 1 and Algorithm 1. In each iteration, the algorithm first feeds current image  $x_{\text{adv}}$  and its label  $t$  to a pre-trained surrogate model  $m$ , where  $x_{\text{adv}}$  is initialized as the benign image and updated subsequently. To optimize  $x_{\text{adv}}$ , we should *maximize* the attack objective loss, which is max-margin logit loss [6] in untargeted attacks and negative cross-entropy loss in targeted ones. The max-margin logit loss is shown in Eq. (1):

$$\mathcal{L}(\hat{y}, t) = \max_{j \neq t} \hat{y}_j - \hat{y}_t \quad (1)$$

where  $\hat{y}$  is the model's logits output of  $x_{\text{adv}}$ ,  $t$  is the true class label  $y$ , and  $j$  indexes the other classes. The negative cross-entropy loss, which is used in the targeted attack, is shown in Eq. (2).

$$\mathcal{L}(\hat{y}, t) = \log\left(\frac{\exp(\hat{y}_t)}{\sum_{j=1}^K \exp(\hat{y}_j)}\right) \quad (2)$$

where  $\hat{y}$  is the model's logits output of  $x_{\text{adv}}$ ,  $t$  is the target class label  $y_{\text{adv}}$  of the targeted attack, and  $j$  enumerates all  $K$  classes. Then, the gradient of the surrogate model  $m$ 's loss w.r.t.  $x_{\text{adv}}$  is computed as  $\hat{g} \leftarrow \nabla_{x_{\text{adv}}} \mathcal{L}(m(x_{\text{adv}}), t)$  (called surrogate gradient). For convenience, we let  $\mathcal{L}(\cdot)$  denote  $\mathcal{L}(f(\cdot), t)$  and  $\bar{g}$  denote the suitable normalization of  $\hat{g}$  under  $\ell_p$  norm constraint as mentioned before. A direct application of PGD with the true gradient  $g$  replaced with  $\hat{g}$  yields the update  $x_{\text{adv}} + \eta \cdot \bar{g}$ . When  $\mathcal{L}(x_{\text{adv}} + \eta \cdot \bar{g}) \geq \mathcal{L}(x_{\text{adv}})$ , we

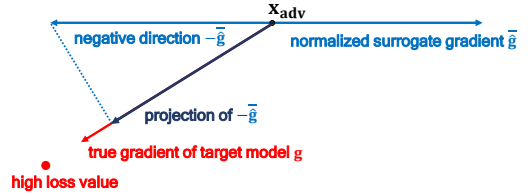


Figure 2: Illustration of SWITCH, where  $x_{\text{adv}}$  is the current image to be updated. When the target model  $f$  is locally approximately linear, the loss should increase along  $-\bar{g}$  direction if it decreases along  $\bar{g}$  direction.

directly accept the update. However, sometimes directly following  $\bar{g}$  may fail to increase the loss because  $\bar{g}$  deviates too much from the true gradient  $g$ . SWITCH proposes to query the loss value to detect such situations in which  $\mathcal{L}(x_{\text{adv}} + \eta \cdot \bar{g}) < \mathcal{L}(x_{\text{adv}})$ .

When following  $\bar{g}$  fails to increase the loss, SWITCH algorithm considers following its opposite direction, namely  $-\bar{g}$ . Its effectiveness is based on the approximate linearity assumption of DNNs [14]. Assuming the target model  $f$  is differentiable at the current point  $x_{\text{adv}}$ , and  $\mathcal{L}(\cdot, t)$  is differentiable at  $f(x_{\text{adv}})$ , then  $\mathcal{L}(f(x_{\text{adv}}), t)$  is differentiable at  $x_{\text{adv}}$ . According to Taylor expansion, we have

$$\mathcal{L}(x_{\text{adv}} + \eta \cdot \bar{g}) = \mathcal{L}(x_{\text{adv}}) + \eta \cdot \bar{g}^\top \nabla \mathcal{L}(x_{\text{adv}}) + o(\eta), \quad (3)$$

where  $\lim_{\eta \rightarrow 0} \frac{o(\eta)}{\eta} = 0$ . Therefore, when  $\eta$  is very small, we have

$$\mathcal{L}(x_{\text{adv}} + \eta \cdot \bar{g}) \approx \mathcal{L}(x_{\text{adv}}) + \eta \cdot \bar{g}^\top \nabla \mathcal{L}(x_{\text{adv}}). \quad (4)$$

According to the approximate linearity assumption, when we set  $\eta$  to be a moderate value, this approximation still holds.

When (4) holds,  $\mathcal{L}(x_{\text{adv}} + \eta \cdot \bar{g}) < \mathcal{L}(x_{\text{adv}})$  corresponds to the case in which  $\eta \cdot \bar{g}^\top \nabla \mathcal{L}(x_{\text{adv}}) < 0$ . By switching the update direction to

the  $-\bar{\mathbf{g}}$ , then we have  $\mathcal{L}(\mathbf{x}_{\text{adv}} - \eta \cdot \bar{\mathbf{g}}) \approx \mathcal{L}(\mathbf{x}_{\text{adv}}) - \eta \cdot \bar{\mathbf{g}}^\top \nabla \mathcal{L}(\mathbf{x}_{\text{adv}}) > \mathcal{L}(\mathbf{x}_{\text{adv}})$ , which explains the effectiveness of the switch operation. Intuitively, assuming the target model  $f$  is locally linear at the current point  $\mathbf{x}_{\text{adv}}$ , then the loss value increases along the  $-\bar{\mathbf{g}}$  direction if it decreases along the  $\bar{\mathbf{g}}$  direction. Fig. 2 illustrates the reason, since in such cases  $-\bar{\mathbf{g}}$  would have a positive component along the true gradient  $\mathbf{g}$  because the inner product of  $-\bar{\mathbf{g}}$  and  $\mathbf{g}$  is positive.

When  $\mathcal{L}(\mathbf{x}_{\text{adv}} + \eta \cdot \bar{\mathbf{g}}) < \mathcal{L}(\mathbf{x}_{\text{adv}})$ , since  $\eta$  is not infinitesimal or  $|\bar{\mathbf{g}}^\top \nabla \mathcal{L}(\mathbf{x}_{\text{adv}})|$  is very small, the approximate linearity assumption may not hold. It is possible that  $\mathcal{L}(\mathbf{x}_{\text{adv}} - \eta \cdot \bar{\mathbf{g}}) < \mathcal{L}(\mathbf{x}_{\text{adv}})$  as well. Therefore, SWITCH queries the value of  $\mathcal{L}(\mathbf{x}_{\text{adv}} - \eta \cdot \bar{\mathbf{g}})$  to decide whether to follow the proposed opposite direction  $-\bar{\mathbf{g}}$ . If both  $\mathcal{L}(\mathbf{x}_{\text{adv}} + \eta \cdot \bar{\mathbf{g}}) < \mathcal{L}(\mathbf{x}_{\text{adv}})$  and  $\mathcal{L}(\mathbf{x}_{\text{adv}} - \eta \cdot \bar{\mathbf{g}}) < \mathcal{L}(\mathbf{x}_{\text{adv}})$  happen, it means that both  $\bar{\mathbf{g}}$  and  $-\bar{\mathbf{g}}$  cannot lead to a increased loss value. In such tricky situation, our switch strategy is still applicable. We propose two strategies to deal with such situation, namely, SWITCH and SWITCH<sub>RGF</sub>. SWITCH does not seek other directions but still chooses a relatively better direction from  $\bar{\mathbf{g}}$  and  $-\bar{\mathbf{g}}$ . Specifically, SWITCH compares  $\mathcal{L}(\mathbf{x}_{\text{adv}} + \eta \cdot \bar{\mathbf{g}})$  and  $\mathcal{L}(\mathbf{x}_{\text{adv}} - \eta \cdot \bar{\mathbf{g}})$  to identify a better direction between  $\bar{\mathbf{g}}$  and  $-\bar{\mathbf{g}}$ . If  $\mathcal{L}(\mathbf{x}_{\text{adv}} - \eta \cdot \bar{\mathbf{g}}) < \mathcal{L}(\mathbf{x}_{\text{adv}} + \eta \cdot \bar{\mathbf{g}})$ , it means that to switch is even worse than not to switch, then SWITCH still follows the original surrogate gradient  $\bar{\mathbf{g}}$ . Otherwise, it switches to  $-\bar{\mathbf{g}}$  in current iteration.

Although SWITCH selects a relatively better update direction from  $\{\bar{\mathbf{g}}, -\bar{\mathbf{g}}\}$  when  $\mathcal{L}(\mathbf{x}_{\text{adv}} + \eta \cdot \bar{\mathbf{g}}) < \mathcal{L}(\mathbf{x}_{\text{adv}})$  and  $\mathcal{L}(\mathbf{x}_{\text{adv}} - \eta \cdot \bar{\mathbf{g}}) < \mathcal{L}(\mathbf{x}_{\text{adv}})$ , it still leads to a decrease of the loss. Alternatively, in such cases we can try other reasonable updates using more queries such that the loss increases. Thus, we develop an extension of SWITCH called SWITCH<sub>RGF</sub>, which uses RGF to obtain an approximate gradient estimate by using  $q$  queries (e.g.,  $q = 50$ ), and then follows such estimated gradient when both  $\bar{\mathbf{g}}$  and  $-\bar{\mathbf{g}}$  are not helpful. Therefore, we can update the current point so that the surrogate gradient may become useful again while keeping the value of the loss function rising. SWITCH<sub>RGF</sub>'s query efficiency might be lower than that of SWITCH but its attack success rate is much higher. We can understand the advantage of SWITCH<sub>RGF</sub> from another perspective: SWITCH<sub>RGF</sub> can achieve the similar success rate to RGF but with an unprecedented low number of queries, because it saves the amount of queries used to estimate the gradient in those attack iterations when the surrogate gradient is useful. For example, it can reduce the query number from 50 RGF queries to only one or two queries in these iterations.

## 4 EXPERIMENT

### 4.1 Experiment Setting

**Datasets and Target Models.** Three datasets, namely, CIFAR-10 [23], CIFAR-100 [23], and TinyImageNet [34], are used for the experiments. We randomly select 1,000 tested images from their validation sets for evaluation, all of which are correctly classified by Inception-v3 network [35]. In the CIFAR-10 and CIFAR-100 datasets, we follow Yan *et al.* [39] to select the following target models: (1) a 272-layers PyramidNet+Shakedrop network (PyramidNet-272) [17, 38] trained using AutoAugment [10]; (2) a model obtained through a neural architecture search called GDAS [12]; (3) a wide

---

### Algorithm 1 SWITCH Attack under $\ell_p$ norm constraint

---

**Input:** Input image  $\mathbf{x}$ , true label  $t$  of  $\mathbf{x}$  (untargeted attack) or target class  $t$  (targeted attack), feed-forward function of the target model  $f$ , feed-forward function of the surrogate model  $m$ , attack objective loss function  $\mathcal{L}(\cdot, \cdot)$ .

**Parameters:** Image learning rate  $\eta$ , the radius  $\epsilon$  of  $\ell_p$  norm ball,  $p \in \{2, \infty\}$ , RGF parameter  $\delta$ , activate SWITCH<sub>RGF</sub> flag USE<sub>RGF</sub>.

**Output:**  $\mathbf{x}_{\text{adv}}$  that satisfies  $\|\mathbf{x}_{\text{adv}} - \mathbf{x}\|_p \leq \epsilon$ .

```

1: Initialize the adversarial example  $\mathbf{x}_{\text{adv}} \leftarrow \mathbf{x}$ 
2:  $L_{\text{last}} \leftarrow \mathcal{L}(f(\mathbf{x}_{\text{adv}}), t)$ 
3: while not successful do
4:    $\hat{\mathbf{g}} \leftarrow \nabla_{\mathbf{x}_{\text{adv}}} \mathcal{L}(m(\mathbf{x}_{\text{adv}}), t)$ 
5:    $\bar{\mathbf{g}} \leftarrow \frac{\hat{\mathbf{g}}}{\|\hat{\mathbf{g}}\|_2}$  if  $p = 2$ , or  $\bar{\mathbf{g}} \leftarrow \text{sign}(\hat{\mathbf{g}})$  if  $p = \infty$ 
6:    $\mathbf{x}_{\text{temp}} \leftarrow \text{Clip}_\epsilon(\mathbf{x}_{\text{adv}} + \eta \cdot \bar{\mathbf{g}})$ 
7:    $L_1 \leftarrow \mathcal{L}(f(\mathbf{x}_{\text{temp}}), t)$ 
8:   if  $L_1 \geq L_{\text{last}}$  then
9:      $\mathbf{x}_{\text{adv}} \leftarrow \mathbf{x}_{\text{temp}}$ ,  $L_{\text{last}} \leftarrow L_1$   $\triangleright$  accept  $\mathbf{x}_{\text{temp}}$  directly
10:  else  $\triangleright$  consider switching gradient direction
11:     $\mathbf{x}'_{\text{temp}} \leftarrow \text{Clip}_\epsilon(\mathbf{x}_{\text{adv}} - \eta \cdot \bar{\mathbf{g}})$ 
12:     $L_2 \leftarrow \mathcal{L}(f(\mathbf{x}'_{\text{temp}}), t)$ 
13:    if  $L_2 \geq L_{\text{last}}$  then
14:       $\mathbf{x}_{\text{adv}} \leftarrow \mathbf{x}'_{\text{temp}}$ ,  $L_{\text{last}} \leftarrow L_2$   $\triangleright$  switch
15:    else
16:      if USERGF then
17:         $\hat{\mathbf{g}}_{\text{RGF}} \leftarrow \frac{1}{q} \sum_{i=1}^q \left( \frac{\mathcal{L}(f(x+\delta u_i), t) - \mathcal{L}(f(x), t)}{\delta} \cdot u_i \right)$ 
18:         $\mathbf{x}_{\text{adv}} \leftarrow \text{Clip}_\epsilon(\mathbf{x}_{\text{adv}} + \eta \cdot \hat{\mathbf{g}}_{\text{RGF}})$ 
19:         $L_{\text{last}} \leftarrow \mathcal{L}(f(\mathbf{x}_{\text{adv}}), t)$ 
20:      else
21:        if  $L_2 \geq L_1$  then
22:           $\mathbf{x}_{\text{adv}} \leftarrow \mathbf{x}'_{\text{temp}}$ ,  $L_{\text{last}} \leftarrow L_2$   $\triangleright$  switch
23:        else
24:           $\mathbf{x}_{\text{adv}} \leftarrow \mathbf{x}_{\text{temp}}$ ,  $L_{\text{last}} \leftarrow L_1$   $\triangleright$  not switch
25:        end if
26:      end if
27:    end if
28:  end if
29: end while
30: return  $\mathbf{x}_{\text{adv}}$ 

```

---

**Table 1: Different attack methods adopt different strategies.**

Method	Surrogate Model(s)	Gradient Estimation	Based on Random Search
Bandits [21]	×	✓	×
RGF [31]	×	✓	×
P-RGF [9]	✓	✓	×
PPBA [24]	×	×	✓
Parsimonious [30]	×	×	×
SignHunter [2]	×	×	×
Square Attack [3]	×	×	✓
SWITCH	✓	×	×

residual network with 28 layers and 10 times width expansion (WRN-28) [40]; and (4) a wide residual network with 40 layers (WRN-40) [40]. In the TinyImageNet dataset, we select (1) ResNeXt-101 (32x4d) [37], (2) ResNeXt-101 (64x4d) [37], and (3) DenseNet-121 with a growth rate of 32 [18] as the target models.

**Table 2: The ratio of performing switch operation and the corresponding increased loss in all iterations of attacking 1,000 images of CIFAR-10 and CIFAR-100 datasets.  $L_{\text{switched}} > L_{\text{last}}$  ratio: The ratio of samples with  $L_{\text{switched}}$  larger than the loss of previous iteration ( $L_{\text{last}}$ ).  $L_{\text{switched}} > L_{\text{xtemp}}$  ratio: the ratio of samples with  $L_{\text{switched}}$  larger than the loss of  $\mathbf{x}_{\text{temp}}$  that produced by using the surrogate gradient before switching.**

Attack Type	Dataset	Norm	switch ratio				$L_{\text{switched}} > L_{\text{last}}$ ratio				$L_{\text{switched}} > L_{\text{xtemp}}$ ratio			
			PyramidNet-272	GDAS	WRN-28	WRN-40	PyramidNet-272	GDAS	WRN-28	WRN-40	PyramidNet-272	GDAS	WRN-28	WRN-40
untargeted	CIFAR-10	$\ell_2$	62.0%	56.1%	60.5%	57.3%	59.8%	66.7%	60.4%	68.9%	94.7%	96.6%	93.3%	95.6%
		$\ell_\infty$	54.8%	51.1%	52.7%	52.2%	72.6%	77.7%	80.0%	83.0%	98.2%	98.8%	98.6%	99.0%
	CIFAR-100	$\ell_2$	52.9%	51.8%	52.7%	54.9%	74.1%	74.4%	73.7%	69.4%	95.5%	97.6%	97.5%	97.0%
		$\ell_\infty$	51.0%	49.8%	50.6%	50.8%	86.7%	92.3%	90.9%	86.4%	98.9%	99.9%	99.4%	98.8%
targeted	CIFAR-10	$\ell_2$	75.9%	74.2%	73.2%	73.4%	48.8%	51.0%	47.0%	53.3%	88.0%	88.5%	88.3%	90.2%
		$\ell_\infty$	79.6%	77.9%	75.9%	77.6%	60.4%	58.7%	58.5%	60.6%	96.2%	96.3%	95.1%	96.3%
	CIFAR-100	$\ell_2$	77.7%	76.2%	78.2%	78.1%	53.0%	56.0%	54.9%	53.5%	87.5%	88.7%	88.1%	87.2%
		$\ell_\infty$	83.2%	80.1%	83.7%	82.4%	66.8%	66.3%	66.9%	61.0%	95.8%	96.4%	96.3%	94.1%

**Table 3: The attack success rates, the average queries, and the average cosine similarities between the surrogate and true gradients with different surrogate models. We perform SWITCH under  $\ell_2$  norm to break a WRN-28 network on the CIFAR-10 dataset. “Random” represents using a random vector from the normal distribution as the surrogate gradient in each iteration.**

Attack Type	Metric	Random	VGG-19(BN)	ResNet-50	ResNet-110	PreResNet-110	ResNeXT-101(8×64d)	ResNeXT-101(16×64d)	DenseNet-100	DenseNet-190
Untargeted	Success Rate	81.8%	96.5%	97.4%	97.5%	95.8%	97.7%	96.1%	96.1%	98.6%
	Avg. Query	751	98	103	147	113	81	63	116	48
	cosine grad	0.026	0.11	0.117	0.108	0.138	0.226	0.235	0.221	0.184
Targeted	Success Rate	50.9%	82.8%	89.3%	87.5%	84.5%	87.4%	80.1%	86.9%	91.8%
	Avg. Query	1537	891	698	809	807	768	765	713	429
	cosine grad	0.022	0.086	0.093	0.085	0.104	0.182	0.189	0.135	0.131

**Method Setting.** In  $\ell_2$  norm attacks, the maximum distortion  $\epsilon$  is set to 1.0 on CIFAR-10 and CIFAR-100, and 2.0 on TinyImageNet. In  $\ell_\infty$  norm attacks,  $\epsilon$  is set to  $8/255$ . The learning rate  $\eta$  is set based on experimental performance. In  $\ell_2$  norm attacks,  $\eta$  is set to  $\epsilon/10$ . In  $\ell_\infty$  norm attacks,  $\eta$  is set to 0.003 ( $\approx \epsilon/10$ ), except for untargeted attacks on CIFAR-10 and CIFAR-100 in which  $\eta$  is set to 0.01. Surrogate model  $m$  is selected as ResNet-110 on CIFAR-10 and CIFAR-100, and ResNet-101 on TinyImageNet. In targeted attacks, the target class is set to  $y_{adv} = (y + 1) \bmod C$ , where  $y_{adv}$  is the target class,  $y$  is the true class, and  $C$  is the number of classes.

**Compared Methods.** The compared query-based black-box attacks are listed in Tab. 1. It includes Bandits [21], RGF [31], prior-guided RGF (P-RGF) [9], Projection & Probability-driven Black-box Attack (PPBA) [24], Parsimonious [30], SignHunter [2], and Square Attack [3]. These methods consist of different strategies. Bandits, RGF, and P-RGF estimate the approximate gradient to optimize the adversarial example; P-RGF improves query efficiency of RGF by utilizing surrogate models, and uses the same surrogate model  $m$  as our method does; PPBA and Square Attack rely on random search optimization; PPBA utilizes a low-frequency constrained sensing matrix; Parsimonious optimizes a discrete surrogate problem by finding the solution among the vertices of the  $\ell_\infty$  ball. We use the PyTorch [33] framework for all experiments, and the official PyTorch implementations of PPBA, Bandits, SignHunter, and Square Attack are used in the experiments. For experimental consistency, we translate the codes of Parsimonious, RGF, and P-RGF from the official TensorFlow [1] version into the PyTorch version. Parsimonious only supports  $\ell_\infty$  norm attacks. We set the maximum number

of queries to 10,000 in all experiments. We set the same  $\epsilon$  value as our method to limit the perturbation of these attacks. The default parameters of these methods are presented in the supplementary material.

**Evaluation Metric.** Following previous studies [9, 39], we report a successful attack if the attack successfully finds an adversarial example within 10,000 queries. We report the attack success rate and the average/median number of queries over successful attacks. To present more comprehensive metrics, we also report the average and median query over all the samples by setting the queries of failed samples to 10,000 in the supplementary material.

## 4.2 Ablation Study

**The Ratio of Increased Loss with SWITCH.** To inspect the effectiveness of SWITCH, we conduct one-step empirical analysis on CIFAR-10 and CIFAR-100 datasets, *i.e.*, we check whether the loss could be increased or decreased by following the switched gradients. Specifically, we first count the proportion of switch operations performed in all attack iterations (switch ratio). Then, only the samples that are updated by using the switched gradient are sent to the target model to record a loss  $L_{\text{switched}}$ . The ratio of samples with  $L_{\text{switched}}$  larger than the loss of previous iteration ( $L_{\text{last}}$ ) is counted as “ $L_{\text{switched}} > L_{\text{last}}$  ratio”. The ratio of  $L_{\text{switched}} > L_{\text{xtemp}}$  is counted to check whether the switched gradient is better than the gradient before switching, where  $\mathbf{x}_{\text{temp}}$  is the image made by using the surrogate gradient before switching. Results of Tab. 2 show that (1) switching is better than not switching (see  $L_{\text{switched}} > L_{\text{xtemp}}$  ratio); (2) switching gradients are rather effective in optimization, since the

**Table 4: Experimental results of untargeted attack on CIFAR-10 and CIFAR-100 datasets.**

Dataset	Norm	Attack	Attack Success Rate				Avg. Query				Median Query			
			PyramidNet-272	GDAS	WRN-28	WRN-40	PyramidNet-272	GDAS	WRN-28	WRN-40	PyramidNet-272	GDAS	WRN-28	WRN-40
CIFAR-10	$\ell_2$	RGF [31]	100%	98.9%	99.4%	100%	1173	889	1622	1352	1020	667	1173	1071
		P-RGF [9]	100%	99.8%	99.1%	99.6%	853	473	1101	831	666	239	468	428
		Bandits [21]	100%	100%	99.4%	99.7%	692	332	807	665	474	210	334	310
		PPBA [24]	100%	99.9%	97.1%	99.1%	1056	634	1339	1118	833	485	754	734
		SignHunter [2]	97%	85.8%	97.7%	99%	794	512	1209	1038	487	267	595	564
		Square Attack [3]	99.8%	100%	96.6%	98.4%	767	363	866	744	435	160	315	308
		NO SWITCH	39.8%	77.1%	80.5%	82.3%	152	58	39	53	21	12	10	9
		SWITCH	90%	95.5%	97.3%	97.1%	490	121	139	83	67	17	14	13
	SWITCH <sub>RGF</sub>	100%	100%	99.4%	100%	555	326	638	516	369	107	60	27	
	$\ell_\infty$	RGF [31]	98.8%	93.8%	98.7%	99.1%	942	645	1194	960	667	460	663	612
		P-RGF [9]	97.3%	97.9%	97.7%	98%	742	337	703	564	408	128	236	217
		Bandits [21]	99.6%	100%	99.4%	99.9%	1015	391	611	542	560	166	224	228
		PPBA [24]	96.6%	99.5%	96.8%	97.6%	860	334	698	574	322	122	188	196
		Parsimonious [30]	100%	100%	100%	100%	701	345	891	738	523	230	424	375
		SignHunter [2]	99.4%	91.8%	100%	100%	379	253	506	415	189	106	205	188
		Square Attack [3]	100%	100%	99.9%	100%	332	126	403	342	182	54	144	139
NO SWITCH		48.9%	84.3%	89.4%	91.8%	422	147	72	120	12	4	3	3	
SWITCH	77.2%	96%	97.2%	98%	522	133	119	68	29	4	3	3		
SWITCH <sub>RGF</sub>	92.8%	98.2%	97.4%	98.2%	525	143	254	218	161	5	3	3		
CIFAR-100	$\ell_2$	RGF [31]	100%	99.8%	99.6%	99.5%	565	554	876	985	459	408	663	612
		P-RGF [9]	100%	99.8%	99.6%	99.3%	407	281	565	765	280	180	296	356
		Bandits [21]	100%	100%	99.9%	99.6%	188	170	312	325	96	90	148	134
		PPBA [24]	100%	100%	99.8%	99.4%	439	362	623	715	322	280	411	419
		SignHunter [2]	97.5%	94.1%	99.1%	99.1%	293	219	565	586	128	82	183	192
		Square Attack [3]	100%	100%	99.5%	99.2%	217	139	326	372	98	55	120	119
		NO SWITCH	68.5%	84.2%	73.6%	74.7%	113	96	58	63	11	8	11	10
		SWITCH	95.7%	98.5%	96.2%	96.1%	128	85	141	124	19	11	15	17
	SWITCH <sub>RGF</sub>	100%	100%	99.9%	99.7%	241	160	306	395	107	15	66	84	
	$\ell_\infty$	RGF [31]	99.8%	98.8%	99%	99%	389	423	552	627	256	255	357	357
		P-RGF [9]	99.3%	98.7%	97.6%	97.8%	308	238	351	478	147	116	138	181
		Bandits [21]	100%	100%	99.8%	99.8%	266	209	262	260	68	56	106	92
		PPBA [24]	99.6%	99.9%	98.7%	98.6%	251	168	349	279	105	73	128	77
		Parsimonious [30]	100%	100%	100%	99.9%	287	185	383	422	204	103	215	213
		SignHunter [2]	99%	97.3%	99.8%	100%	125	119	211	255	52	37	59	60
		Square Attack [3]	100%	100%	100%	99.8%	76	57	150	162	17	19	46	36
NO SWITCH		81.8%	92.1%	86.4%	87.2%	243	84	126	191	3	3	3	3	
SWITCH	93.4%	97.5%	93.5%	94.3%	145	64	109	91	4	3	4	4		
SWITCH <sub>RGF</sub>	99.3%	98.5%	98.4%	97.7%	136	67	166	144	6	3	4	4		

losses of a large fraction of samples are increased from the last iteration after following the switched gradient ( $L_{\text{switched}} > L_{\text{last}}$ ) even though they have  $L_{\text{temp}} < L_{\text{last}}$ ; (3) targeted attacks perform more switch operations than untargeted ones because their surrogate gradients deviates too much from true gradients.

**Transferability of Gradient Directions.** We study the effects of SWITCH with different surrogate models. Tab. 3 shows the relationship between the query number and the cosine similarity w.r.t. the true gradients. It shows that with a larger cosine similarity, the query efficiency is higher. This is because the a higher cosine similarity implies a more useful surrogate gradient so that the improvement of the loss in each iteration could be larger, thus saving the overall queries. Specifically, the cosine similarity (w.r.t. the true gradient) of the gradient of a surrogate model is significantly larger than that of a random direction, demonstrating the necessity and effectiveness of utilizing the transferable gradient.

**NO SWITCH versus SWITCH versus SWITCH<sub>RGF</sub>.** To validate the effectiveness of the gradient switch operation in terms of the attack success rate, we consider a baseline NO SWITCH which is the algorithm without switching the surrogate gradient.

NO SWITCH consecutively follows the gradient  $\hat{g}$  of the surrogate model  $m$  during the optimization. The results are presented in all the tables of experimental results (Tabs. 4, 5, 6, 7, 8) and Fig. 3. We derive the following conclusions based on these results:

(1) NO SWITCH requires only one query in each attack iteration which is fewer than SWITCH and SWITCH<sub>RGF</sub>, thereby resulting high query efficiency. However, NO SWITCH obtains unsatisfactory attack success rate and its success rate can hardly exceed 90%.

(2) SWITCH and SWITCH<sub>RGF</sub> outperforms NO SWITCH in terms of attack success rate by a large margin. Although SWITCH<sub>RGF</sub> uses the most queries among three SWITCH versions, it significantly surpasses SWITCH in terms of the success rate. Readers can refer to Fig. 3 for more details, which demonstrates SWITCH<sub>RGF</sub> and SWITCH outperform NO SWITCH in different query budgets.

### 4.3 Comparisons with State-of-the-Arts

**Results of Attacks on Normal Models.** Tab. 4 and Tab. 5 show the experimental results of CIFAR-10 and CIFAR-100 datasets. Tab. 6 and Tab. 7 show the results of TinyImageNet dataset. We can conclude the following:

**Table 5: Experimental results of targeted attack under  $\ell_2$  norm constraint on CIFAR-10 and CIFAR-100 datasets.**

Dataset	Attack	Attack Success Rate				Avg. Query				Median Query			
		PyramidNet-272	GDAS	WRN-28	WRN-40	PyramidNet-272	GDAS	WRN-28	WRN-40	PyramidNet-272	GDAS	WRN-28	WRN-40
CIFAR-10	RGF [31]	100%	100%	97.5%	99.8%	1795	1249	2454	2176	1632	1071	2040	1938
	P-RGF [9]	99.9%	100%	97.1%	99.7%	1698	1149	2140	1738	1548	966	1613	1444
	Bandits [21]	96.3%	100%	81.5%	84.2%	1966	905	2092	2088	1426	650	1268	1240
	PPBA [24]	96%	99.8%	82.1%	88.1%	2062	1180	2623	2610	1479	885	1887	1845
	SignHunter [2]	98.9%	99.9%	92.7%	97.3%	1681	1047	1953	1863	1409	791	1510	1480
	Square Attack [3]	95.1%	99.5%	88.8%	93.5%	1700	885	1983	1697	1070	442	1070	1024
	NO SWITCH	14.8%	43.1%	53.2%	56.1%	180	114	73	120	46	28	23	22
	SWITCH	71.4%	89.2%	89.6%	90.7%	1245	526	587	550	296	92	85	78
SWITCH <sub>RGF</sub>	100%	100%	97.6%	99.8%	1146	746	1566	1325	894	482	851	841	
CIFAR-100	RGF [31]	99.9%	99.6%	98.2%	96.2%	1542	1538	2374	2775	1326	1275	1989	2346
	P-RGF [9]	99.9%	99.7%	97.7%	96.1%	1528	1445	2295	2662	1288	1184	1870	2196
	Bandits [21]	97.5%	98.4%	82.3%	82.3%	2063	1620	3003	3200	1418	1080	2204	2344
	PPBA [24]	95.4%	96.4%	82.3%	63.8%	2087	1606	3008	3477	1568	1140	2274	2874
	SignHunter [2]	98.4%	96.4%	91.6%	89.4%	1494	1423	1938	2078	1176	1072	1505	1610
	Square Attack [3]	96.6%	94.2%	87.4%	85.1%	1469	1281	2091	2242	873	707	1250	1468
	NO SWITCH	9.6%	14.6%	11.1%	11.6%	788	622	776	627	65	42	62	64
	SWITCH	73.6%	78%	74.2%	73.5%	997	748	949	1077	309	164	276	313
SWITCH <sub>RGF</sub>	99.9%	99.8%	97.8%	96.4%	1101	992	1743	2078	839	698	1259	1538	

**Table 6: Experimental results of untargeted attacks under  $\ell_2$  norm on TinyImageNet dataset.  $D_{121}$ : DenseNet-121,  $R_{32}$ : ResNeXt-101 (32 $\times$ 4d),  $R_{64}$ : ResNeXt-101 (64 $\times$ 4d).**

Attack	Attack Success Rate			Avg. Query			Median Query		
	$D_{121}$	$R_{32}$	$R_{64}$	$D_{121}$	$R_{32}$	$R_{64}$	$D_{121}$	$R_{32}$	$R_{64}$
RGF [31]	99.4%	94.1%	96.1%	1485	2651	2579	1173	2052	2000
P-RGF [9]	99.5%	94.2%	94.8%	1218	2092	1985	792	1288	1272
Bandits [21]	98.7%	93%	94.6%	1032	2005	1896	576	1198	1184
PPBA [24]	99.7%	96.9%	97.5%	1151	2004	1838	851	1445	1396
SignHunter [2]	97.6%	93%	94.4%	560	1290	1238	188	585	601
Square Attack [3]	98.5%	92.2%	93.6%	566	1287	1164	187	501	416
NO SWITCH	25.6%	17.8%	16.1%	399	641	499	35	44	39
SWITCH	98.6%	97.1%	96.9%	174	307	299	54	75	77
SWITCH <sub>RGF</sub>	99.4%	97.7%	97.4%	1010	1700	1552	640	1003	1000

**Table 7: Experimental results of targeted attack under  $\ell_2$  norm on TinyImageNet dataset.  $D_{121}$ : DenseNet-121,  $R_{32}$ : ResNeXt-101 (32 $\times$ 4d),  $R_{64}$ : ResNeXt-101 (64 $\times$ 4d).**

Attack	Attack Success Rate			Avg. Query			Median Query		
	$D_{121}$	$R_{32}$	$R_{64}$	$D_{121}$	$R_{32}$	$R_{64}$	$D_{121}$	$R_{32}$	$R_{64}$
RGF [31]	87.6%	71.6%	75.9%	3735	4845	4821	3264	4335	4386
P-RGF [9]	84.1%	67.9%	72.1%	3714	4584	4620	3252	4148	4212
Bandits [21]	56.4%	36.8%	36.6%	3907	4229	4503	3586	3818	4236
PPBA [24]	70.1%	50.3%	51.9%	3734	4256	4488	3120	3887	4111
SignHunter [2]	85.3%	67.4%	72.2%	2650	3342	3412	1914	2663	2901
Square Attack [3]	70.1%	49.3%	53.9%	2595	3287	3391	1777	2541	2603
NO SWITCH	4.3%	3.5%	3.6%	889	201	610	69	62	98
SWITCH	74.7%	68.4%	68.5%	1241	1453	1532	536	538	610
SWITCH <sub>RGF</sub>	83%	71.1%	75.8%	3486	4111	4150	2880	3603	3710

(1) In untargeted  $\ell_2$  attacks, SWITCH usually achieves similar success rates to other state-of-the-art attacks with much fewer queries. In  $\ell_\infty$  attacks and targeted attacks, the success rates of SWITCH are worse than those of untargeted ones. However, SWITCH features fast initial convergence, which manifests its advantage in

**Table 8: Experimental results of attacking defensive models under  $\ell_\infty$  norm constraint on the TinyImageNet dataset, where CD is ComDefend [22] and FD is Feature Distillation [26]. All defensive models adopt ResNet-50 as the backbone.**

Attack	Attack Success Rate			Avg. Query		
	CD [22]	FD [26]	JPEG [16]	CD [22]	FD [26]	JPEG [16]
RGF [31]	31.3%	10.2%	3.2%	2446	2433	2552
P-RGF [9]	37.3%	25.2%	10.2%	1946	1958	2605
Bandits [21]	39.6%	12.5%	8.1%	893	1272	1698
PPBA [24]	18.3%	72.9%	48%	528	1942	2387
Parsimonious [30]	83.9%	99.5%	96.1%	866	359	410
SignHunter [2]	87.6%	40.3%	99.5%	208	558	260
Square Attack [3]	36.1%	99.5%	97.9%	57	167	301
NO SWITCH	55.9%	40%	45.8%	757	843	634
SWITCH	92.5%	93.2%	80%	365	353	698
SWITCH <sub>RGF</sub>	74.7%	69.7%	43.6%	1448	1723	2442

those attacks under the setting of extremely limited queries. Meanwhile, SWITCH<sub>RGF</sub> makes up the shortcoming of SWITCH and raises the success rate to a high level.

(3) SWITCH<sub>RGF</sub> consumes significant fewer queries than RGF, and also than P-RGF even though they use the same surrogate model, because the amount of queries used to estimate gradients are saved in those iterations when the surrogate gradient is useful. **Results of Attacks on Defensive Models.** To inspect the performance of attacking defensive models, we conduct the experiments of attacking three defensive models, *i.e.*, ComDefend (CD) [22], Feature Distillation (FD) [26], and JPEG [16]. CD is a defensive model that consists of a compression CNN and a reconstruction CNN to transform the adversarial image to defend against attacks. FD is a DNN-oriented compression defensive framework. JPEG is a image transformation-based defensive method. All the defensive models adopt the backbone of ResNet-50. Results of Tab. 8 conclude:

(1) SWITCH achieves the best success rate in attacking CD among all attacks, and it also achieves the comparable success rate with state-of-the-art attacks in attacking FD.



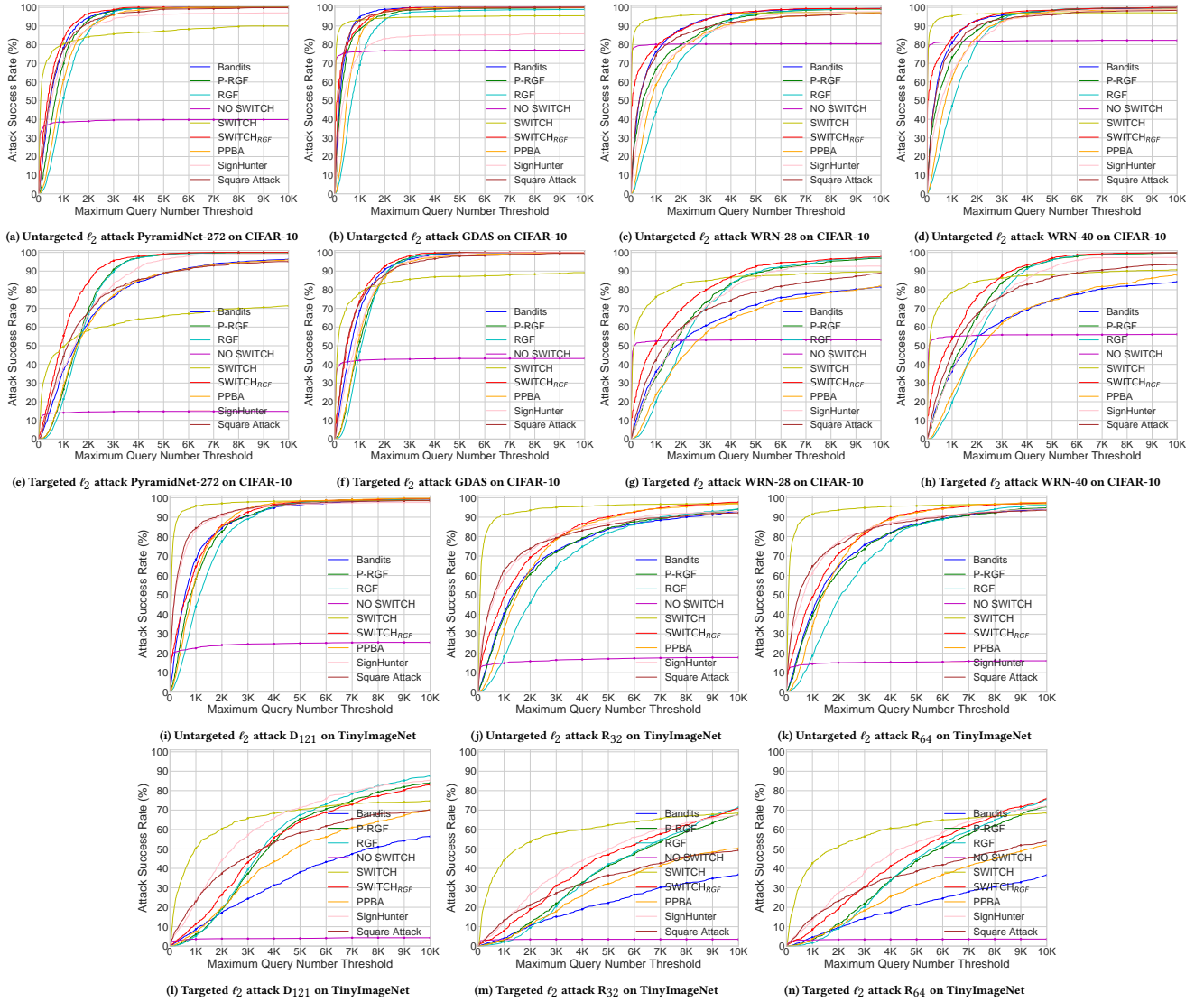


Figure 3: Detailed comparisons of attack success rates at different maximum limited queries, where  $D_{121}$  is DenseNet-121,  $R_{32}$  is ResNeXt-101 (32x4d) and  $R_{64}$  is ResNeXt-101 (64x4d).

(2) SWITCH outperforms  $SWITCH_{RGF}$  because gradient estimates obtained from RGF is almost useless in attacking these defensive models, possibly due to the phenomenon of obfuscated gradients [4]. Readers can refer to success rates of RGF in Tab. 8. **Attack Success Rates at Different Maximum Queries.** To investigate the results more comprehensively, we present the attack success rates by limiting different maximum query numbers in Fig. 3. It shows that (1) SWITCH is rather useful for the attack scenario with an extremely low query limitation. In the difficult targeted attacks (row 2 and row 4), SWITCH exhibits the highest success rate under 1,000 limited queries. This is because of the skillful use of the exploring direction (surrogate gradient  $\pm \bar{g}$ ), which is more effective than those attacks that follow random directions (e.g., Square Attack), resulting in SWITCH’s fast initial convergence.

In real scenarios, the query budgets are often extremely limited, making SWITCH more useful in these situations. (2) SWITCH may converge to a lower success rate given a large query number threshold, which is a drawback of SWITCH. However,  $SWITCH_{RGF}$  avoids this problem while often remains the superior query efficiency.

## 5 CONCLUSION

In this study, we propose a highly efficient black-box attack named SWITCH. It exploits the gradient of a surrogate model and then switches it if following such gradient cannot improve the value of attack objective function. We also develop an extension called  $SWITCH_{RGF}$  to further improve the success rate. Despite the simplicity of our proposed methods, the strategy is effective and explainable, and extensive experiments demonstrate that our proposed methods achieve state-of-the-art performance.



## REFERENCES

- [1] Martín Abadi, Paul Barham, Jianmin Chen, Zhifeng Chen, Andy Davis, Jeffrey Dean, Matthieu Devin, Sanjay Ghemawat, Geoffrey Irving, Michael Isard, et al. 2016. Tensorflow: A system for large-scale machine learning. In *12th {USENIX} Symposium on Operating Systems Design and Implementation ({OSDI} 16)*. 265–283.
- [2] Abdullah Al-Dujaili and Una-May O’Reilly. 2020. Sign Bits Are All You Need for Black-Box Attacks. In *International Conference on Learning Representations*. <https://openreview.net/forum?id=SygW0TEFwH>
- [3] Maksym Andriushchenko, Francesco Croce, Nicolas Flammarion, and Matthias Hein. 2020. Square Attack: A Query-Efficient Black-Box Adversarial Attack via Random Search. In *Computer Vision – ECCV 2020*, Andrea Vedaldi, Horst Bischof, Thomas Brox, and Jan-Michael Frahm (Eds.). Springer International Publishing, Cham, 484–501.
- [4] Anish Athalye, Nicholas Carlini, and David Wagner. 2018. Obfuscated Gradients Give a False Sense of Security: Circumventing Defenses to Adversarial Examples. In *Proceedings of the 35th International Conference on Machine Learning (Proceedings of Machine Learning Research)*, Jennifer Dy and Andreas Krause (Eds.), Vol. 80. PMLR, Stockholm, Sweden, 274–283. <http://proceedings.mlr.press/v80/athalye18a.html>
- [5] Arjun Nitin Bhagoji, Warren He, Bo Li, and Dawn Song. 2018. Practical black-box attacks on deep neural networks using efficient query mechanisms. In *European Conference on Computer Vision*. Springer, 158–174.
- [6] Nicholas Carlini and David Wagner. 2017. Towards evaluating the robustness of neural networks. In *2017 IEEE Symposium on Security and Privacy (SP)*. IEEE, 39–57.
- [7] Pin-Yu Chen, Huan Zhang, Yash Sharma, Jinfeng Yi, and Cho-Jui Hsieh. 2017. Zoo: Zeroth order optimization based black-box attacks to deep neural networks without training substitute models. In *Proceedings of the 10th ACM Workshop on Artificial Intelligence and Security*. ACM, 15–26.
- [8] Minhao Cheng, Simranjit Singh, Pin-Yu Chen, Sijia Liu, and Cho-Jui Hsieh. 2020. Sign-OPT: A Query-Efficient Hard-label Adversarial Attack. (2020). <https://openreview.net/forum?id=SkITQCNtvs>
- [9] Shuyu Cheng, Yinpeng Dong, Tianyu Pang, Hang Su, and Jun Zhu. 2019. Improving Black-box Adversarial Attacks with a Transfer-based Prior. In *Advances in Neural Information Processing Systems*, Vol. 32. Curran Associates, Inc. <https://proceedings.neurips.cc/paper/2019/file/32508f53f24c46f685870a075eaa29c-Paper.pdf>
- [10] Ekin D. Cubuk, Barret Zoph, Dandelion Mane, Vijay Vasudevan, and Quoc V. Le. 2019. AutoAugment: Learning Augmentation Strategies From Data. In *Proceedings of the IEEE/CVF Conference on Computer Vision and Pattern Recognition (CVPR)*.
- [11] Ambra Demontis, Marco Melis, Maura Pintor, Matthew Jagielski, Battista Biggio, Alina Oprea, Cristina Nita-Rotaru, and Fabio Roli. 2019. Why Do Adversarial Attacks Transfer? Explaining Transferability of Evasion and Poisoning Attacks. In *28th USENIX Security Symposium (USENIX Security 19)*. USENIX Association, Santa Clara, CA, 321–338. <https://www.usenix.org/conference/usenixsecurity19/presentation/demontis>
- [12] Xuanyi Dong and Yi Yang. 2019. Searching for a robust neural architecture in four gpu hours. In *Proceedings of the IEEE Conference on Computer Vision and Pattern Recognition*. 1761–1770.
- [13] Yinpeng Dong, Hang Su, Baoyuan Wu, Zhifeng Li, Wei Liu, Tong Zhang, and Jun Zhu. 2019. Efficient decision-based black-box adversarial attacks on face recognition. In *Proceedings of the IEEE Conference on Computer Vision and Pattern Recognition*. 7714–7722.
- [14] Ian Goodfellow, Jonathon Shlens, and Christian Szegedy. 2015. Explaining and Harnessing Adversarial Examples. In *International Conference on Learning Representations*. <http://arxiv.org/abs/1412.6572>
- [15] Chuan Guo, Jacob Gardner, Yurong You, Andrew Gordon Wilson, and Kilian Weinberger. 2019. Simple Black-box Adversarial Attacks. In *Proceedings of the 36th International Conference on Machine Learning (Proceedings of Machine Learning Research)*, Kamalika Chaudhuri and Ruslan Salakhutdinov (Eds.), Vol. 97. PMLR, 2484–2493. <http://proceedings.mlr.press/v97/guo19a.html>
- [16] Chuan Guo, Mayank Rana, Moustapha Cisse, and Laurens van der Maaten. 2018. Countering Adversarial Images using Input Transformations. In *International Conference on Learning Representations*. <https://openreview.net/forum?id=SyJ7CIWcb>
- [17] Dongyoon Han, Jiwhan Kim, and Junmo Kim. 2017. Deep pyramidal residual networks. In *Proceedings of the IEEE conference on computer vision and pattern recognition*. 5927–5935.
- [18] Gao Huang, Zhuang Liu, Laurens van der Maaten, and Kilian Q. Weinberger. 2017. Densely Connected Convolutional Networks. In *The IEEE Conference on Computer Vision and Pattern Recognition (CVPR)*.
- [19] Qian Huang, Isay Katsman, Horace He, Zeqi Gu, Serge Belongie, and Ser-Nam Lim. 2019. Enhancing adversarial example transferability with an intermediate level attack. In *Proceedings of the IEEE International Conference on Computer Vision*. 4733–4742.
- [20] Andrew Ilyas, Logan Engstrom, Anish Athalye, and Jessy Lin. 2018. Black-box Adversarial Attacks with Limited Queries and Information. In *Proceedings of the 35th International Conference on Machine Learning (Proceedings of Machine Learning Research)*, Jennifer Dy and Andreas Krause (Eds.), Vol. 80. PMLR, 2137–2146. <http://proceedings.mlr.press/v80/ilyas18a.html>
- [21] Andrew Ilyas, Logan Engstrom, and Aleksander Madry. 2019. Prior Convictions: Black-box Adversarial Attacks with Bandits and Priors. In *International Conference on Learning Representations*. <https://openreview.net/forum?id=BkMiWhr5K7>
- [22] Xiaojun Jia, Xingxing Wei, Xiaochun Cao, and Hassan Foroosh. 2019. ComDefend: An efficient image compression model to defend adversarial examples. In *Proceedings of the IEEE Conference on Computer Vision and Pattern Recognition*. 6084–6092.
- [23] Alex Krizhevsky, Geoffrey Hinton, et al. 2009. Learning multiple layers of features from tiny images. (2009).
- [24] Jie Li, Rongrong Ji, Hong Liu, Jianzhuang Liu, Bineng Zhong, Cheng Deng, and Qi Tian. 2020. Projection & Probability-Driven Black-Box Attack. In *Proceedings of the IEEE Conference on Computer Vision and Pattern Recognition (CVPR)*.
- [25] Yanpei Liu, Xinyun Chen, Chang Liu, and Dawn Song. 2017. Delving into Transferable Adversarial Examples and Black-box Attacks. In *Proceedings of 5th International Conference on Learning Representations*.
- [26] Zihao Liu, Qi Liu, Tao Liu, Nuo Xu, Xue Lin, Yanzhi Wang, and Wujie Wen. 2019. Feature distillation: Dnn-oriented jpeg compression against adversarial examples. In *2019 IEEE/CVF Conference on Computer Vision and Pattern Recognition (CVPR)*. IEEE, 860–868.
- [27] Chen Ma, Li Chen, and Junhai Yong. 2021. Simulating Unknown Target Models for Query-Efficient Black-box Attacks. In *Proceedings of the IEEE Conference on Computer Vision and Pattern Recognition (CVPR)*.
- [28] Chen Ma, Chenxu Zhao, Hailin Shi, Li Chen, Junhai Yong, and Dan Zeng. 2019. MetaAdvDet: Towards Robust Detection of Evolving Adversarial Attacks. In *Proceedings of the 27th ACM International Conference on Multimedia (MM ’19)*. Association for Computing Machinery, New York, NY, USA, 692–701. <https://doi.org/10.1145/3343031.3350887>
- [29] Aleksander Madry, Aleksandar Makelov, Ludwig Schmidt, Dimitris Tsipras, and Adrian Vladu. 2018. Towards Deep Learning Models Resistant to Adversarial Attacks. In *International Conference on Learning Representations*. <https://openreview.net/forum?id=rjZiBfZAb>
- [30] Seungyong Moon, Gaon An, and Hyun Oh Song. 2019. Parsimonious Black-Box Adversarial Attacks via Efficient Combinatorial Optimization. In *International Conference on Machine Learning (ICML)*.
- [31] Yurii Nesterov and Vladimir Spokoiny. 2017. Random gradient-free minimization of convex functions. *Foundations of Computational Mathematics* 17, 2 (2017), 527–566.
- [32] Nicolas Papernot, Patrick McDaniel, and Ian Goodfellow. 2016. Transferability in machine learning: from phenomena to black-box attacks using adversarial samples. *arXiv preprint arXiv:1605.07277* (2016).
- [33] Adam Paszke, Sam Gross, Francisco Massa, Adam Lerer, James Bradbury, Gregory Chanan, Trevor Killeen, Zeming Lin, Natalia Gimelshein, Luca Antiga, et al. 2019. PyTorch: An imperative style, high-performance deep learning library. In *Advances in Neural Information Processing Systems*. 8024–8035.
- [34] Olga Russakovsky, Jia Deng, Hao Su, Jonathan Krause, Sanjeev Satheesh, Sean Ma, Zhiheng Huang, Andrej Karpathy, Aditya Khosla, Michael Bernstein, et al. 2015. Imagenet large scale visual recognition challenge. *International journal of computer vision* 115, 3 (2015), 211–252.
- [35] Christian Szegedy, Vincent Vanhoucke, Sergey Ioffe, Jon Shlens, and Zbigniew Wojna. 2016. Rethinking the inception architecture for computer vision. In *Proceedings of the IEEE conference on computer vision and pattern recognition*. 2818–2826.
- [36] Chun-Chen Tu, Paishun Ting, Pin-Yu Chen, Sijia Liu, Huan Zhang, Jinfeng Yi, Cho-Jui Hsieh, and Shin-Ming Cheng. 2019. Autozoom: Autoencoder-based zeroth order optimization method for attacking black-box neural networks. In *Proceedings of the AAAI Conference on Artificial Intelligence*, Vol. 33. 742–749.
- [37] Saining Xie, Ross Girshick, Piotr Dollár, Zhuowen Tu, and Kaiming He. 2017. Aggregated residual transformations for deep neural networks. In *Proceedings of the IEEE conference on computer vision and pattern recognition*. 1492–1500.
- [38] Y. Yamada, M. Iwamura, T. Akiba, and K. Kise. 2019. Shakedown Regularization for Deep Residual Learning. *IEEE Access* 7 (2019), 186126–186136. <https://doi.org/10.1109/ACCESS.2019.2960566>
- [39] Ziang Yan, Yiwen Guo, and Changshui Zhang. 2019. Subspace Attack: Exploiting Promising Subspaces for Query-Efficient Black-box Attacks. In *Advances in Neural Information Processing Systems*. 3820–3829.
- [40] Sergey Zagoruyko and Nikos Komodakis. 2016. Wide Residual Networks. In *Proceedings of the British Machine Vision Conference (BMVC)*, Edwin R. Hancock Richard C. Wilson and William A. P. Smith (Eds.). BMVA Press, Article 87, 12 pages. <https://doi.org/10.5244/C.30.87>

## Supplementary Material

### A EXPERIMENTAL SETTINGS

#### A.1 Hyperparameters of Compared Methods

**RGF and P-RGF attack.** Hyperparameters of RGF [31] and P-RGF [9] attacks are listed in Tab. 9. The experiments of RGF and P-RGF are conducted by using the PyTorch version translated from the official TensorFlow implementation.

**Table 9: The hyperparameters of RGF and P-RGF attacks.**

Norm	Hyperparameter	Value
$\ell_2$	$h$ , image learning rate	0.1
	$\sigma$ , sampling variance	1e-4
$\ell_\infty$	$h$ , image learning rate	0.005
	$\sigma$ , sampling variance	1e-4
$\ell_2, \ell_\infty$	surrogate model used in CIFAR-10/100	ResNet-110
$\ell_2, \ell_\infty$	surrogate model used in TinyImageNet	ResNet-101

**Bandits.** Hyperparameters of Bandits [21] are listed in Tab. 10. The OCO learning rate is used to update the prior, where the prior is an alias of gradient  $\mathbf{g}$  for updating the input image.

**Parsimonious.** Hyperparameters of Parsimonious [30] are listed in Tab. 11. Parsimonious only supports  $\ell_\infty$  norm attack. We follow the official implementation to set the initial block size to 4 in all experiments.

**SignHunter.** Hyperparameters of SignHunter [2] are listed in Tab. 12.

**Square Attack.** Hyperparameters of Square Attack [3] are shown in Tab. 13. Square Attack randomly samples a square window filled with perturbations in each iteration. The area of this square window in the first iteration is initialized as  $H \times W \times p$ , which is then reduced in subsequent iterations.

**Table 10: The hyperparameters of Bandits.**

Norm	Hyperparameter	Value
$\ell_2$	$\delta$ , finite difference probe	0.01
	$\eta$ , image learning rate	0.1
	$\eta_g$ , OCO learning rate	0.1
	$\tau$ , Bandits exploration	0.3
	maximum query times	10,000
	$\ell_\infty$	$\delta$ , finite difference probe
$\eta$ , image learning rate		1/255
$\eta_g$ , OCO learning rate		1.0
$\tau$ , Bandits exploration		0.3
maximum query times		10,000

**PPBA.** Hyperparameters of Projection & Probability-driven Black-box Attack (PPBA) [24] are shown in Tab. 14. We follow the official implementation to initialize the random matrix (strided) with the dimension of 1,500.

**Table 11: The hyperparameters of Parsimonious.**

Hyperparameter	Value
the number of iterations in local search	1
$k$ , initial block size	4
batch size	64
no hierarchical evaluation	False

**Table 12: The hyperparameters of SignHunter.**

Hyperparameter	Value
$\epsilon$ , radius of $\ell_2$ norm ball in CIFAR-10/100	1.0
$\epsilon$ , radius of $\ell_2$ norm ball in TinyImageNet	2.0
$\epsilon$ , maximum radius of $\ell_\infty$ norm ball	8/255

**Table 13: The hyperparameters of Square Attack.**

Hyperparameter	Value
$p$ , initial probability of changing a coordinate	0.05

**Table 14: The hyperparameters of PPBA.**

Dataset	Hyperparameter	Value
CIFAR-10/100	order	strided
	$\rho$ , the change of measurement vector $z$ for $\ell_\infty$ norm attack	0.001
	$\rho$ , the change of measurement vector $z$ for $\ell_2$ norm attack	0.01
	$\mu$ , the momentum of calculating effective probability	1
	frequency dim, used in initialize blocks	11
	low-frequency dimension	1,500
	stride, used in initialize blocks	7
	number of samples per iteration	1
	TinyImageNet	order
$\rho$ , the change of measurement vector $z$ for $\ell_\infty$ norm attack		0.001
$\rho$ , the change of measurement vector $z$ for $\ell_2$ norm attack		0.01
$\mu$ , the momentum of calculating effective probability		1
frequency dim, used in initialize block		15
low-frequency dimension		1,500
stride, used in initialize block		7
number of samples per iteration		1

**SWITCH.** Hyperparameters of the proposed SWITCH are listed in Tab. 15. The configurations of the surrogate model used in SWITCH is the pre-trained ResNet-110 in CIFAR-10 and CIFAR-100 datasets, and ResNet-101 in TinyImageNet dataset.

**Table 16: Experimental results of untargeted attack under  $\ell_2$  norm on TinyImageNet dataset.  $D_{121}$ : DenseNet-121,  $R_{32}$ : ResNeXt-101 (32×4d),  $R_{64}$ : ResNeXt-101 (64×4d). We include failed samples in the computation of the average and median query, and the query numbers of failed samples are set to 10,000.**

Attack	Attack Success Rate			Avg. Query			Median Query		
	$D_{121}$	$R_{32}$	$R_{64}$	$D_{121}$	$R_{32}$	$R_{64}$	$D_{121}$	$R_{32}$	$R_{64}$
RGF [31]	99.4%	94%	96.1%	1536	3085	2868	1173	2193	2094
P-RGF [9]	99.5%	94.1%	94.8%	1262	2551	2402	794	1402	1376
Bandits [21]	98.7%	93%	94.6%	1148	2565	2333	585	1333	1271
PPBA [24]	99.7%	96.9%	97.5%	1178	2252	2042	853	1511	1440
SignHunter [2]	97.6%	93%	94.4%	786	1900	1728	204	673	658
Square Attack [3]	98.5%	92.2%	93.6%	707	1966	1730	196	600	485
NO SWITCH	25.6%	17.8%	16.1%	7542	8334	8470	10000	10000	10000
SWITCH	98.6%	97.1%	96.9%	311	588	599	56	77	79
SWITCH <sub>RGF</sub>	99.4%	97.7%	97.4%	1064	1891	1772	663	1047	1056

**Table 17: Experimental results of untargeted attack under  $\ell_\infty$  norm on TinyImageNet dataset.  $D_{121}$ : DenseNet-121,  $R_{32}$ : ResNeXt-101 (32×4d),  $R_{64}$ : ResNeXt-101 (64×4d). We include failed samples in the computation of the average and median query, and the query numbers of failed samples are set to 10,000.**

Attack	Attack Success Rate			Avg. Query			Median Query		
	$D_{121}$	$R_{32}$	$R_{64}$	$D_{121}$	$R_{32}$	$R_{64}$	$D_{121}$	$R_{32}$	$R_{64}$
RGF [31]	96.4%	85.3%	87.4%	1465	3251	3084	715	1639	1588
P-RGF [9]	94.5%	83.9%	85.9%	1384	2938	2768	468	968	954
Bandits [21]	99.2%	94.1%	95.3%	1036	2224	2054	532	1040	1075
PPBA [24]	99.6%	97.9%	98.2%	441	1116	979	192	425	401
Parsimonious [30]	100%	99.3%	99.3%	273	708	644	190	301	287
SignHunter [2]	99.5%	98.6%	99%	250	713	621	59	125	156
Square Attack [3]	100%	99.4%	99.6%	160	454	417	74	160	143
NO SWITCH	49.3%	33.4%	33.4%	5431	6918	6898	10000	10000	10000
SWITCH	93.1%	85.7%	85.4%	948	1880	1891	73	132	148
SWITCH <sub>RGF</sub>	98.3%	92.9%	94%	1165	2204	2011	534	951	1002

**Table 18: Experimental results of targeted attack under  $\ell_2$  norm on TinyImageNet dataset.  $D_{121}$ : DenseNet-121,  $R_{32}$ : ResNeXt-101 (32×4d),  $R_{64}$ : ResNeXt-101 (64×4d). We include failed samples in the computation of the average and median query, and the query numbers of failed samples are set to 10,000.**

Attack	Attack Success Rate			Avg. Query			Median Query		
	$D_{121}$	$R_{32}$	$R_{64}$	$D_{121}$	$R_{32}$	$R_{64}$	$D_{121}$	$R_{32}$	$R_{64}$
RGF [31]	87.5%	71.4%	75.5%	4512	6309	6069	3570	6248	5661
P-RGF [9]	84%	67.7%	71.9%	4714	6323	6121	3782	6406	5838
Bandits [21]	56.4%	36.8%	36.6%	6563	7876	7988	7533	10000	10000
PPBA [24]	70.1%	50.3%	51.9%	5608	7111	7140	4787	9794	9322
SignHunter [2]	85.3%	67.4%	72.2%	3731	5512	5243	2395	5005	4374
Square Attack [3]	70.1%	49.3%	53.9%	4809	6691	6438	3568	10000	8570
NO SWITCH	4.3%	3.5%	3.6%	9608	9657	9662	10000	10000	10000
SWITCH	74.7%	68.4%	68.5%	3457	4154	4200	983	1548	1781
SWITCH <sub>RGF</sub>	83%	71.1%	75.8%	4593	5813	5566	3549	5456	5164

**Table 15: The hyperparameters of SWITCH attack.**

Norm	Hyperparameter	Value
$\ell_2$	$\eta$ , image learning rate for CIFAR-10 & CIFAR-100	0.1
	$\eta$ , image learning rate for TinyImageNet	0.2
$\ell_\infty$	$\eta$ , image learning rate for untargeted attack in CIFAR-10 & CIFAR-100	0.01
	$\eta$ , image learning rate for targeted attack in CIFAR-10 & CIFAR-100	0.003
	$\eta$ , image learning rate in TinyImageNet dataset	0.003
$\ell_2, \ell_\infty$	$m$ , surrogate model used in CIFAR-10 & CIFAR-100 dataset	ResNet-110
$\ell_2, \ell_\infty$	$m$ , surrogate model used in TinyImageNet dataset	ResNet-101

## B EXPERIMENTAL RESULTS

**Experimental Results Including Failed Examples.** In our original paper, we report the experimental results (attack success rate and the average/median number of queries) over successful attacks, the samples of failed attacks are excluded in the statistics. To present the results more comprehensively, we also report the average and median query over all the samples by setting the queries of failed samples to 10,000 in this supplementary material. The experimental results are shown in Tab. 16, Tab. 17, Tab. 18, Tab. 19, and Tab. 20. We can draw the following conclusions based on the results of these tables.

(1) The number of the average and median query depends on the attack success rate. If the success rate is low such that the queries of many samples are set to 10,000, then the average query is low. If the success rate is below 50%, then the median query is 10,000.

(2) Compared to the results of the average and median query in the original paper, the average and the median query of SWITCH is lower than NO SWITCH because its attack success rate is higher than NO SWITCH.

**Attack Success Rates at Different Maximum Queries.** Fig. 4, Fig. 5, and Fig. 6 show the attack success rates by limiting different maximum queries in each example.

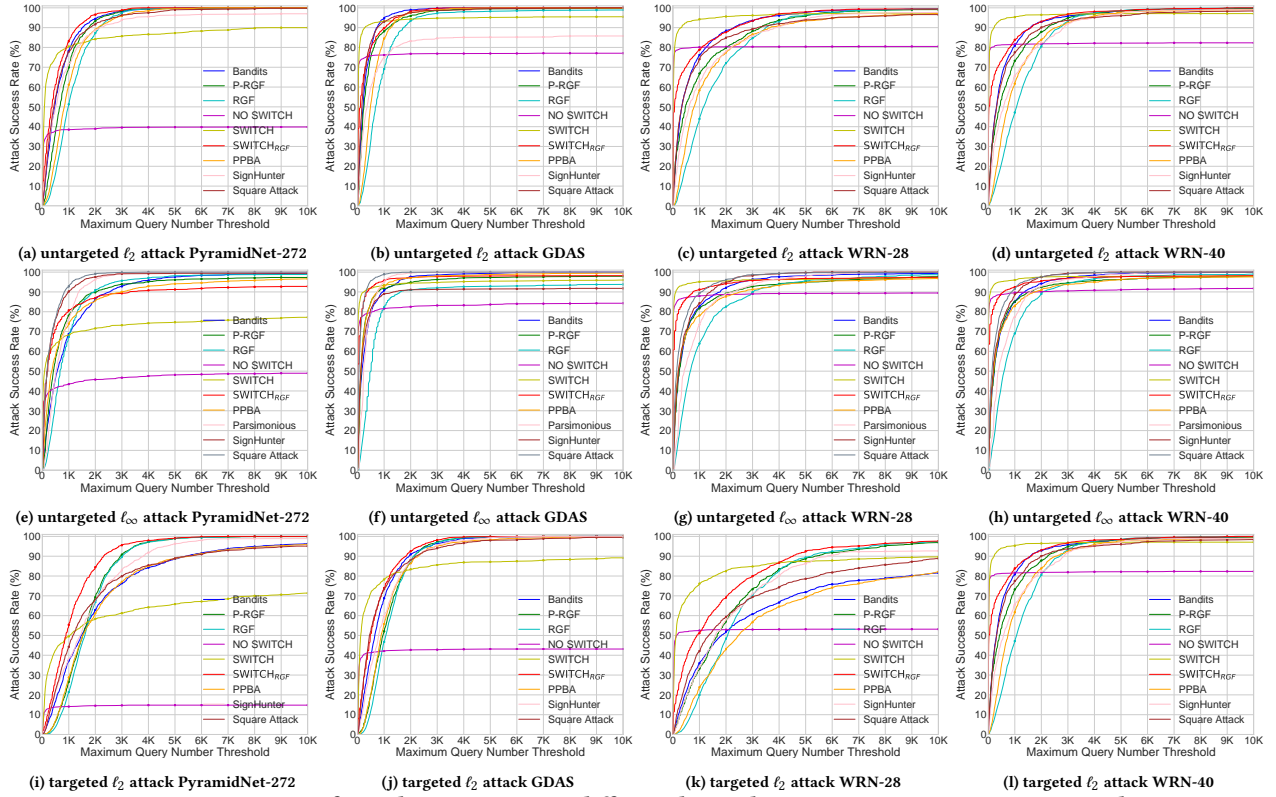
**Histogram of Query Numbers.** To observe the distribution of query numbers in more detail, Fig. 7, Fig. 8, Fig. 9 show the histograms of query numbers in CIFAR-10, CIFAR-100, TinyImageNet. To draw the histogram, we separate the range of query number into 10 intervals to count the number of samples in each interval separately, and the intervals are separated by the vertical lines of figures. Each bar indicates one attack, and the height of each bar indicates the number of samples with the queries belong to this query interval. The results show that the highest red bars (SWITCH) are always located in the low query number’s area, thereby confirming that most adversarial examples of SWITCH have the fewest queries.

**Table 19: Experimental results of untargeted attack on CIFAR-10 and CIFAR-100 datasets. We include failed samples in the computation of the average and median query, and the query numbers of failed samples are set to 10,000.**

Dataset	Norm	Attack	Attack Success Rate				Avg. Query				Median Query			
			PyramidNet-272	GDAS	WRN-28	WRN-40	PyramidNet-272	GDAS	WRN-28	WRN-40	PyramidNet-272	GDAS	WRN-28	WRN-40
CIFAR-10	$\ell_2$	RGF [31]	100%	98.9%	99.4%	100%	1173	989	1672	1352	1020	714	1173	1071
		P-RGF [9]	100%	99.8%	99.1%	99.6%	853	492	1182	868	666	240	470	432
		Bandits [21]	100%	100%	99.4%	99.7%	692	332	862	693	474	210	336	313
		PPBA [24]	100%	99.9%	97.1%	99.1%	1056	643	1591	1199	833	486	801	739
		SignHunter [2]	97%	85.8%	97.7%	99%	1070	1861	1412	1128	510	358	614	579
		Square Attack [3]	99.8%	100%	96.6%	98.4%	786	363	1178	893	436	160	331	313
		NO SWITCH	39.8%	77.1%	80.5%	82.3%	6077	2337	1982	1811	10000	16	12	11
		SWITCH	90%	95.5%	97.3%	97.1%	1442	566	407	371	83	19	15	13
		SWITCH <sub>RGF</sub>	100%	100%	99.4%	100%	555	326	695	516	369	107	61	28
	$\ell_\infty$	RGF [31]	98.8%	93.8%	98.7%	99%	1051	1225	1309	1042	669	510	663	612
		P-RGF [9]	97.3%	97.9%	97.7%	98%	992	540	918	754	420	132	239	232
		Bandits [21]	99.6%	100%	99.4%	99.9%	1051	391	667	551	564	166	226	228
		PPBA [24] [24]	96.6%	99.5%	96.8%	97.6%	1171	382	997	801	361	123	199	203
		Parsimonious [30]	100%	100%	100%	100%	701	345	891	738	523	230	424	375
		SignHunter [2]	99.4%	91.8%	100%	100%	436	1053	506	415	191	122	205	188
		Square Attack [3]	100%	100%	99.9%	100%	332	126	412	342	182	54	145	140
		NO SWITCH	48.9%	84.3%	89.4%	91.8%	5311	1696	1119	933	10000	5	3	3
		SWITCH	77.2%	96%	97.2%	98%	2685	528	397	267	89	5	3	3
SWITCH <sub>RGF</sub>	92.8%	98.2%	97.4%	98.2%	1207	321	509	394	209	5	3	3		
CIFAR-100	$\ell_2$	RGF [31]	100%	99.8%	99.6%	99.5%	565	573	913	1031	459	408	663	612
		P-RGF [9]	100%	99.8%	99.6%	99.3%	407	301	603	830	280	180	302	356
		Bandits [21]	100%	100%	99.9%	99.6%	188	170	322	365	96	90	148	136
		PPBA [24]	100%	100%	99.8%	99.4%	439	362	642	771	323	280	412	423
		SignHunter [2]	97.5%	94.1%	99.1%	99.1%	539	797	650	672	138	95	187	194
		Square Attack [3]	100%	100%	99.5%	99.2%	217	139	375	450	98	55	123	122
		NO SWITCH	68.5%	84.2%	73.6%	74.7%	3225	1657	2684	2577	20	11	16	14
		SWITCH	95.7%	98.5%	96.2%	96.1%	548	229	519	514	20	11	16	17
		SWITCH <sub>RGF</sub>	100%	100%	99.9%	99.7%	241	160	316	424	107	15	66	87
	$\ell_\infty$	RGF [31]	99.8%	98.8%	99%	99%	409	542	647	721	256	255	357	357
		P-RGF [9]	99.3%	98.7%	97.6%	97.8%	377	369	585	690	153	116	156	182
		Bandits [21]	100%	100%	99.8%	99.8%	266	209	282	280	68	57	108	92
		PPBA [24] [24]	99.6%	99.9%	98.7%	98.6%	290	178	476	417	106	73	129	80
		Parsimonious [30]	100%	100%	100%	99.9%	287	185	383	432	204	103	215	213
		SignHunter [2]	99%	97.3%	99.8%	100%	225	385	230	255	53	39	59	60
		Square Attack [3]	100%	100%	100%	99.8%	76	57	150	182	17	19	46	37
		NO SWITCH	81.8%	92.1%	86.4%	87.2%	2020	866	1470	1442	5	3	4	4
		SWITCH	93.4%	97.5%	93.5%	94.3%	793	311	747	652	5	3	4	4
SWITCH <sub>RGF</sub>	99.3%	98.5%	98.4%	97.7%	206	212	324	374	6	3	5	4		

**Table 20: Experimental results of targeted attack under  $\ell_2$  norm constraint on CIFAR-10 and CIFAR-100 datasets. We include failed samples in the computation of the average and median query, and the query numbers of failed samples are set to 10,000.**

Dataset	Attack	Attack Success Rate				Avg. Query				Median Query			
		PyramidNet-272	GDAS	WRN-28	WRN-40	PyramidNet-272	GDAS	WRN-28	WRN-40	PyramidNet-272	GDAS	WRN-28	WRN-40
CIFAR-10	RGF [31]	100%	100%	97.4%	99.8%	1795	1249	2643	2191	1632	1071	2091	1938
	P-RGF [9]	99.9%	100%	96.9%	99.7%	1706	1149	2369	1762	1548	966	1668	1444
	Bandits [21]	96.3%	100%	81.5%	84.2%	2264	905	3554	3335	1478	650	1824	1673
	PPBA [24]	96%	99.8%	82.1%	88.1%	2380	1198	3943	3493	1535	887	2474	2190
	SignHunter [2]	98.9%	99.9%	92.7%	97.3%	1772	1056	2543	2083	1427	793	1590	1536
	Square Attack [3]	95.1%	99.5%	88.8%	93.5%	2107	931	2877	2239	1162	449	1355	1140
	NO SWITCH	14.8%	43.1%	53.2%	56.1%	8545	5735	4722	4455	10000	10000	144	88
	SWITCH	71.4%	89.2%	89.6%	90.7%	3752	1550	1562	1432	1042	121	116	97
SWITCH <sub>RGF</sub>	100%	100%	97.6%	99.8%	1146	746	1769	1343	894	482	900	842	
CIFAR-100	RGF [31]	99.9%	99.6%	98.2%	96.2%	1550	1573	2513	3053	1326	1275	2040	2397
	P-RGF [9]	99.9%	99.6%	97.7%	96.1%	1537	1472	2474	2952	1288	1185	1874	2278
	Bandits [21]	97.5%	98.4%	82.3%	62.3%	2263	1751	4245	5761	1469	1106	2989	5658
	PPBA [24]	95.4%	96.4%	82.3%	63.8%	2447	1911	4249	5840	1643	1189	2914	5606
	SignHunter [2]	98.4%	96.4%	91.6%	89.4%	1632	1734	2613	2920	1190	1107	1684	1866
	Square Attack [3]	96.6%	94.2%	87.4%	85.1%	1763	1788	3088	3397	925	777	1649	1898
	NO SWITCH	9.6%	14.6%	11.1%	11.6%	9114	8628	8977	8909	10000	10000	10000	10000
	SWITCH	73.6%	78%	74.2%	73.5%	3375	2782	3284	3444	751	347	662	790
SWITCH <sub>RGF</sub>	99.9%	99.8%	97.8%	96.4%	1110	1011	1926	2367	839	699	1288	1587	


**Figure 4: Comparison of attack success rate at different limited maximum queries on CIFAR-10 dataset.**

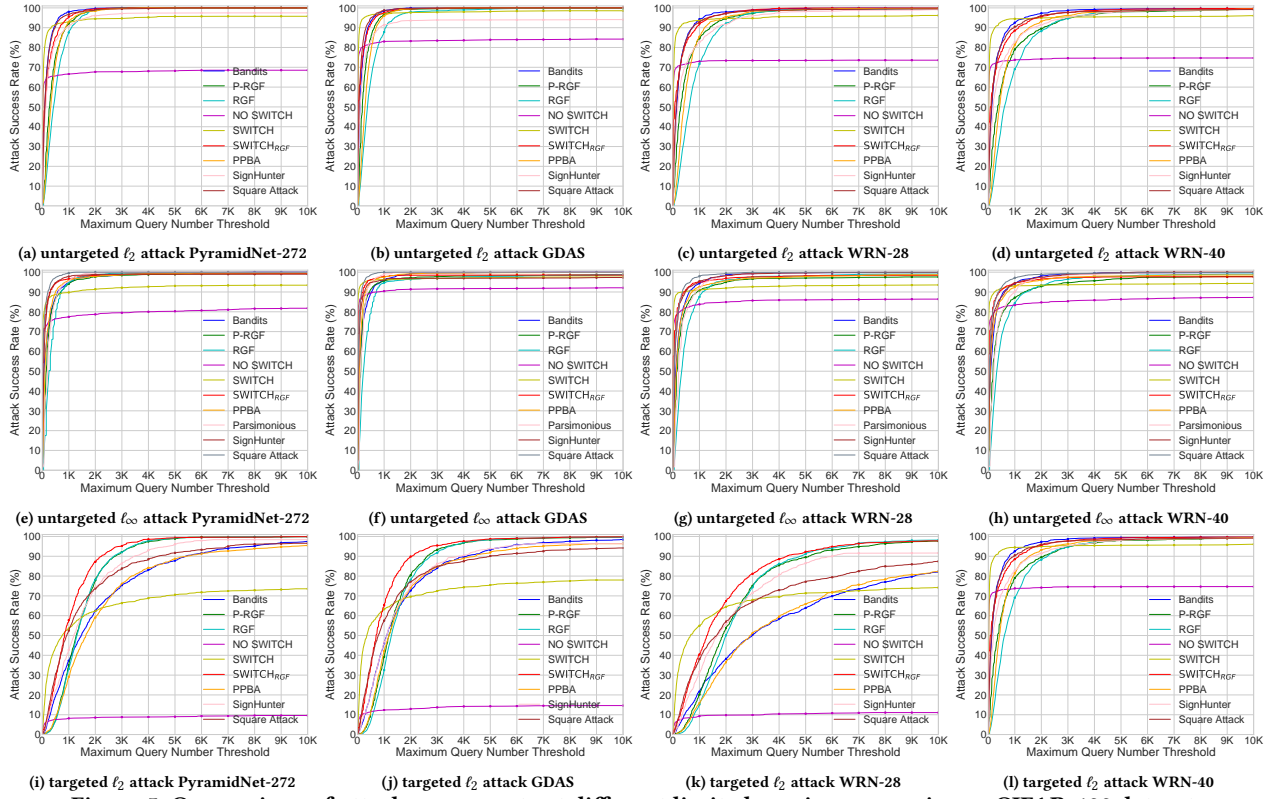


Figure 5: Comparison of attack success rate at different limited maximum queries on CIFAR-100 dataset.

Switching Transferable Gradient Directions for Query-Efficient Black-Box Adversarial Attacks

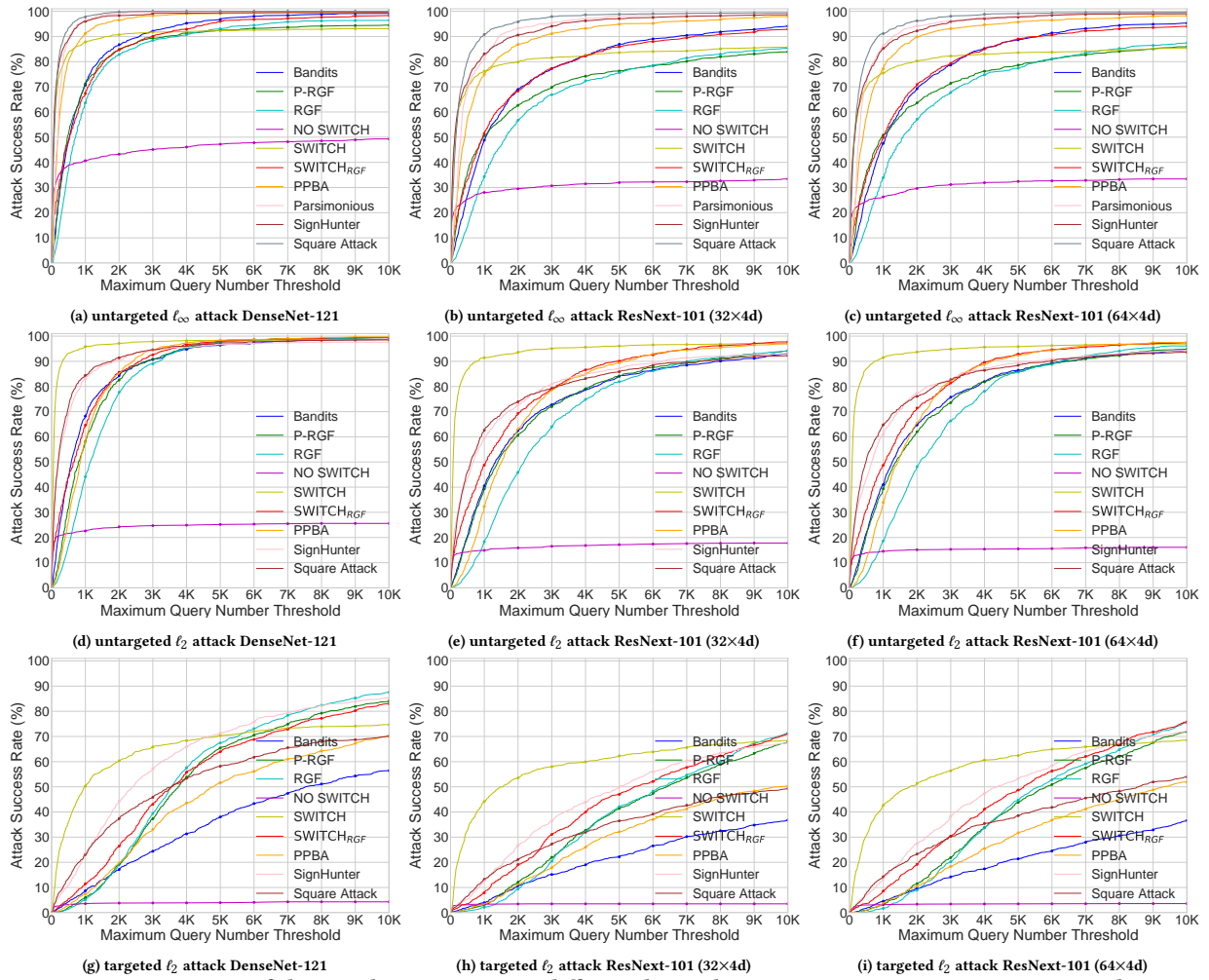


Figure 6: Comparison of the attack success rate at different limited maximum queries in TinyImageNet dataset.



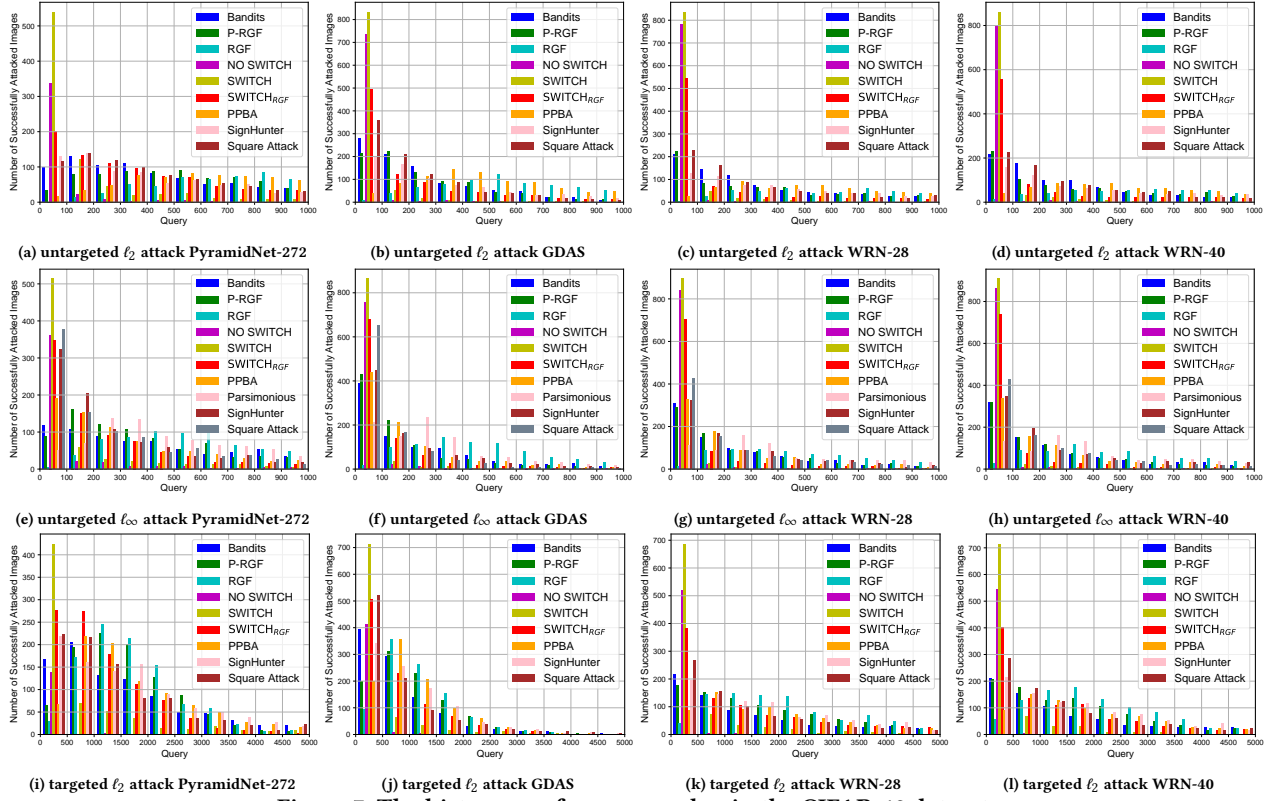


Figure 7: The histogram of query number in the CIFAR-10 dataset.

# Switching Transferable Gradient Directions for Query-Efficient Black-Box Adversarial Attacks

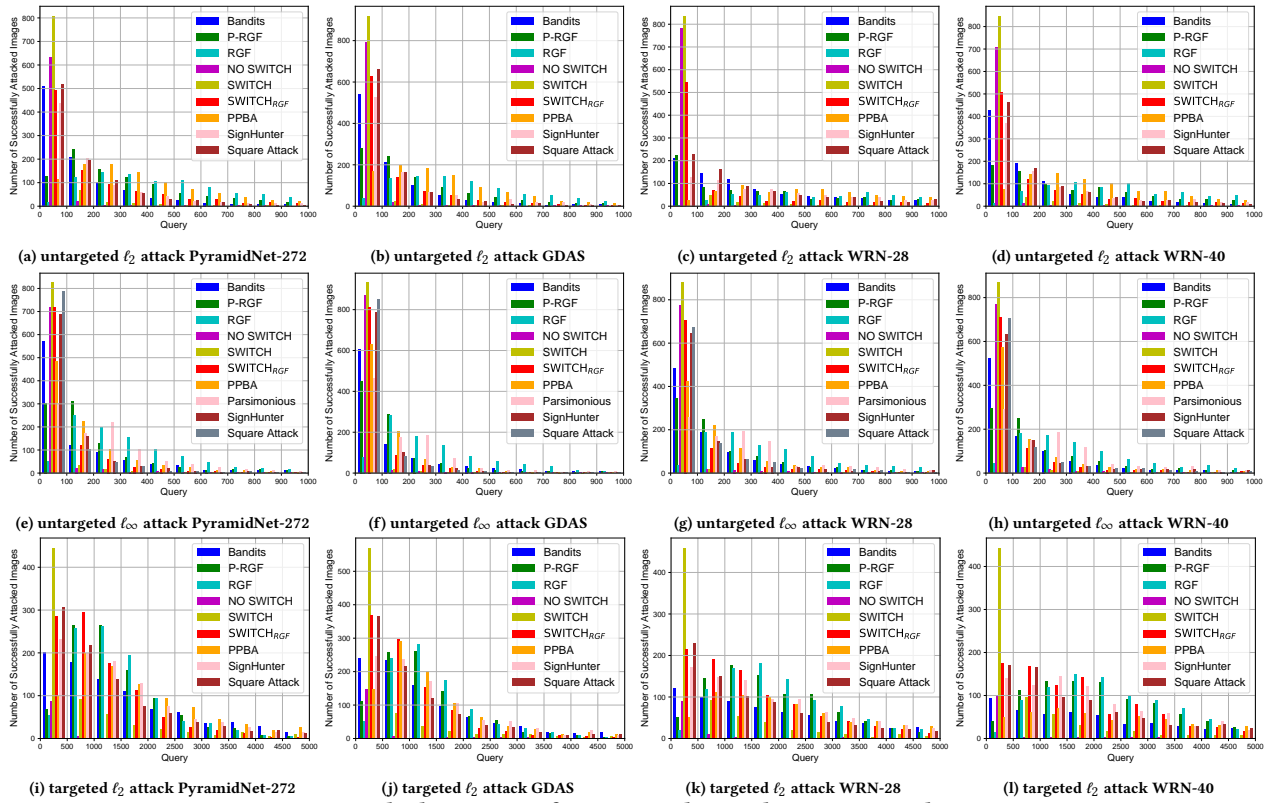


Figure 8: The histogram of query number in the CIFAR-100 dataset.

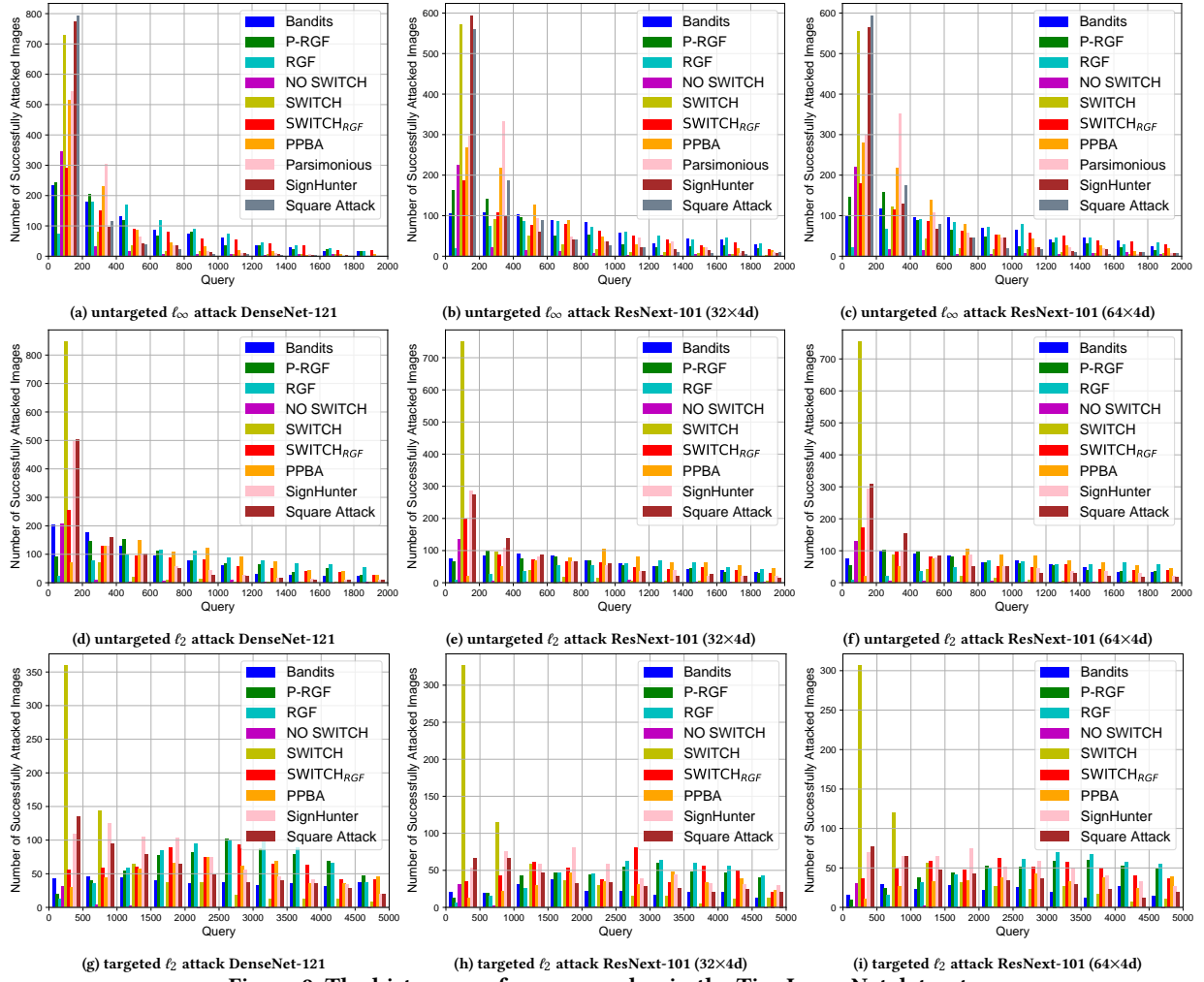


Figure 9: The histogram of query number in the TinyImageNet dataset.